

Accepted Manuscript

Title: NH_3 -SCR reaction mechanisms of $\text{NbO}_x/\text{Ce}_{0.75}\text{Zr}_{0.25}\text{O}_2$
catalyst: DRIFTS and kinetics studies

Author: Ziran Ma Xiaodong Wu Hanna Härelind Duan Weng
Baodong Wang Zhichun Si



PII: S1381-1169(16)30245-X
DOI: <http://dx.doi.org/doi:10.1016/j.molcata.2016.06.023>
Reference: MOLCAA 9929

To appear in: *Journal of Molecular Catalysis A: Chemical*

Received date: 4-5-2016
Revised date: 23-6-2016
Accepted date: 24-6-2016

Please cite this article as: Ziran Ma, Xiaodong Wu, Hanna Härelind, Duan Weng, Baodong Wang, Zhichun Si, NH_3 -SCR reaction mechanisms of $\text{NbO}_x/\text{Ce}_{0.75}\text{Zr}_{0.25}\text{O}_2$ catalyst: DRIFTS and kinetics studies, *Journal of Molecular Catalysis A: Chemical* <http://dx.doi.org/10.1016/j.molcata.2016.06.023>

This is a PDF file of an unedited manuscript that has been accepted for publication. As a service to our customers we are providing this early version of the manuscript. The manuscript will undergo copyediting, typesetting, and review of the resulting proof before it is published in its final form. Please note that during the production process errors may be discovered which could affect the content, and all legal disclaimers that apply to the journal pertain.

NH₃-SCR reaction mechanisms of NbO_x/Ce_{0.75}Zr_{0.25}O₂ catalyst: DRIFTS and kinetics studies

Ziran Ma^{a,b,1}, Xiaodong Wu^{a,*,1}, Hanna Härelind^c, Duan Weng^{a,d}, Baodong Wang^{b,*},
Zhichun Si^d

^a *The Key Laboratory of Advanced Materials of Ministry of Education, School of Materials Science and Engineering, Tsinghua University, Beijing 100084, China*

^b *National Institute of Clean-and-Low-Carbon Energy (NICE), Beijing 102209, China*

^c *Competence Centre for Catalysis, Dept. of Chemistry and Chemical Engineering, Chalmers University of Technology, SE-412 96 Göteborg, Sweden*

^d *Advanced Materials Institute, Graduate School at Shenzhen, Tsinghua University, Shenzhen 518055, China*

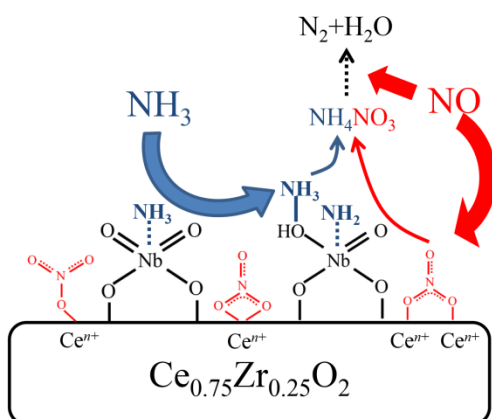
* Corresponding author. Tel.: +86 10 62792375

E-mail address: wuxiaodong@tsinghua.edu.cn (X. Wu), wangbaodong@nicenergy.com (B. Wang)

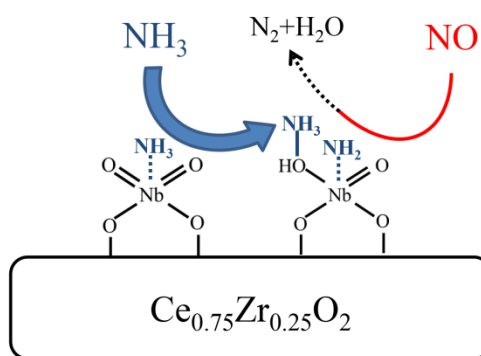
¹ These two authors contributed equally to this work.

Graphical Abstract:

At low temperatures



At high temperatures



Highlights:

- 1) $\text{NbO}_x/\text{Ce}_{0.75}\text{Zr}_{0.25}\text{O}_2$ catalyst shows high NH_3 -SCR activity in a broad temperature window.
- 2) Reaction mechanisms on NbCZ catalyst are verified by DRIFTS and kinetic studies.
- 3) “L-H” and “E-R” mechanisms are presented for NbCZ in different temperature ranges.
- 4) The $\text{NH}_4\text{NO}_3+\text{NO}$ reaction is accelerated over NbCZ catalyst at low temperatures.
- 5) The NH_2+NO reaction is also promoted by addition of niobia at high temperatures.

Abstract:

A $\text{NbO}_x/\text{Ce}_{0.75}\text{Zr}_{0.25}\text{O}_2$ (NbCZ) catalyst was synthesized by a citric acid-aided sol-gel method. It shows that above 80% NO_x conversion and above 95% N_2 selectivity for the selective catalytic reduction of NO_x by ammonia over this catalyst are achieved in the temperature range 200-450 °C. Based on the DRIFTS and kinetic studies over NbCZ and $\text{Ce}_{0.75}\text{Zr}_{0.25}\text{O}_2$, the promotion mechanism by niobia loading was elucidated with an overall reaction pathway. Two different reaction routes, “L-H” mechanism via “ $\text{NH}_4\text{NO}_3+\text{NO}$ ” at low temperatures (< 200 °C) and “E-R” mechanism via “ NH_2+NO ” at high temperatures (> 350 °C), are presented. The niobia addition increases the surface acidity and promotes the formation of nitrates species at low temperatures. In this way, the reaction between the ads- NH_3 and nitrates species is accelerated to form NH_4NO_3 intermediates, which then decompose to N_2 and H_2O . The reaction of the ads- NH_3 species with gaseous NO_x at high temperatures is also promoted due to the enhanced acidity and weakened thermal stability of nitrates after niobia loading.

Keywords: CeO₂-ZrO₂ mixed oxides, Niobia modification, NH₃-SCR, Mechanism, DRIFTS

1. Introduction

Selective catalytic reduction with ammonia is an effective technique for the abatement of NO_x from diesel exhaust and stationary sources. To meet stringent legislations, $\text{V}_2\text{O}_5\text{-WO}_3/\text{TiO}_2$ catalyst has been commercially applied in these fields for decades [1, 2]. However, some drawbacks still remain for vanadium-based catalysts, including the narrow operation temperature window (300-400 °C), toxicity and volatility of V_2O_5 species and the poor N_2 selectivity in the high temperature range due to significant N_2O formation. To avoid such problems, many researchers have been taking persistent efforts to develop novel and environmentally friendly catalysts with high NO_x conversion, high N_2 selectivity and nontoxic species.

Ceria and ceria-containing materials have been widely employed as catalysts because of the facile redox cycling between Ce^{3+} and Ce^{4+} . The acid-base properties, nontoxicity and lower cost of ceria also make them promising candidates for $\text{NH}_3\text{-SCR}$ catalysts. Recently, many solid-acid modified Ce based catalysts have been reported, such as $\text{CeO}_2\text{-WO}_3$ [3-9], $\text{CeO}_2\text{-Nb}_2\text{O}_5$ [10-15], $\text{CeO}_2\text{-MoO}_3$ [16-22], $\text{CeO}_2\text{-PO}_4^{3-}$ [23-26] and $\text{CeO}_2\text{-SO}_4^{2-}$ [27-30]. Among them, $\text{CeO}_2\text{-Nb}_2\text{O}_5$ based catalyst appears to be very promising due to its superior low-temperature activity, wide operation temperature window and acceptable resistances to SO_2 and alkali metals. The $\text{NH}_3\text{-SCR}$ mechanisms over solid acid-ceria catalysts have been studied by some researchers. Chen et al. [3, 4] presented that the addition of tungsten oxide to CeO_2 catalyst can promote the NO oxidation to NO_2 , with which the adsorbed NH_3 species react readily to generate N_2 and H_2O via an Eley-Rideal (E-R) mechanism. The reaction of the adsorbed NH_3 and nitrates species according to the Langmuir-Hinshelwood (L-H) mechanism is another crucial reaction route on $\text{CeO}_2\text{-WO}_x$ catalyst. This mechanism is later supported by Peng et al. [8] based on *in-situ* DRIFTS and *in-situ* Raman techniques. They proposed that $\text{CeO}_2\text{-WO}_x$ catalyst follow a double-separated acid and redox cycle, in which tungsta and ceria played critical roles, respectively. A similar “E-R” mechanism was presented as the main reaction mechanism by Zhu et al. [16] on M_xO_y ($\text{M}=\text{Ni}$, Cu and Fe)/ $\text{MoO}_3/\text{CeO}_2$ catalyst. They thought that the NH_3 or NH_4^+ species adsorbed on different acid sites are activated through deprotonation process (partial oxidation) to form NH_2 (amide) or NH_3^+ species. These activated species react with the gas phase NO subsequently to form a NH_2NO nitrosamide species, from which N_2 and H_2O are produced. Liu et al. [20] suggested that over

CeO₂-MoO_x catalyst, both adsorbed NH₃ and weakly adsorbed NO₂, could participate in “L-H” mechanism at low temperatures. At high temperatures, coordinated NH₃ species combine with gaseous NO, forming an intermediate which would finally decompose to H₂O and N₂. In the study of Yu et al. [25], it was proposed that the SCR reaction over Zr₃(PO₄)₂/CeO₂-ZrO₂ proceeds via the combination of the adjacent surface N_xO_y species and ads-NH₃ species via a “L-H” mechanism. In summary, some common reaction routes were presented for solid acid-ceria catalysts.

Investigations on the mechanism of CeO₂-Nb₂O₅ based catalyst have been rarely reported. Casapu et al. [10] found that the slightly lower stability of the N_xO_y adsorbed species on the MnNbCe surface as well as the larger amount of NO₂ evolved at low temperature represents an important effect of the niobium addition to the MnCe catalyst. Qu et al [13] suggested that the abundance of surface adsorbed oxygen might arise from the short-range activation effect of niobium oxide species to cerium oxide species. Recently, they pointed out that the SCR reaction pathway over the Ce-Nb catalysts may follow both the “E-R” and “L-H” mechanisms, where the former contributed more especially at high reaction temperatures [15]. Similarly, our previous study [14] also observed the enhanced NH₃ activation and NO₃⁻ formation, and the subsequent promoted reaction of ads-NH₃ and ads-NO₃⁻ species for the SCR reaction over NbO_x/CeO₂-ZrO₂ catalysts according to the “L-H” mechanism. At high temperatures, the thermal stability of the adsorbed NO₃⁻ species are reduced significantly, and thus the SCR reaction on this catalyst mainly follows the “E-R” mechanism via the reaction of ads-NH₂ species and gaseous NO. However, the detailed reaction routes of CeO₂-NbO_x based catalysts remain to be studied. More *in-situ* DRIFTS and kinetics studies would be very beneficial to help us to elucidate the aspects by niobia modification in the surface properties of ceria based catalysts and propose the specific reaction mechanisms of the modified catalysts at different temperatures.

2. Experimental

2.1. Catalyst preparation

Ce_{0.75}Zr_{0.25}O₂ (CZ) catalyst was synthesized by a citric acid-aided sol-gel method using Ce(NO₃)₄·6H₂O and Zr(NO₃)₄·5H₂O as the precursors according to the procedure reported in Ref.

[14]. The resultant gel was dried at 110 °C overnight and then subjected to decomposition at 300 °C for 1 h and calcination at 550 °C for 3 h under air at ambient conditions. The $\text{NbO}_x/\text{Ce}_{0.75}\text{Zr}_{0.25}\text{O}_2$ (NbCZ) catalyst was subsequently synthesized by impregnating the as-received $\text{Ce}_{0.75}\text{Zr}_{0.25}\text{O}_2$ powders with $\text{C}_{12}\text{H}_7\text{NbO}_{24}$ solution, with the impregnated powders dried at 110 °C overnight and calcined at 550 °C for 3 h in static air. The loading amount of niobia was 15 wt.%. For comparison, CZ was also treated through the above calcination procedure.

2.2. Activity measurement

The measurements of the steady-state activity were carried out in a fixed-bed quartz reactor (inner diameter 10 mm) under the following conditions: 200 mg sample with 60-80 mesh, 500 ppm NH_3 , 500 ppm NO , 5% O_2 , 12% CO_2 , 5% H_2O (when used), N_2 as balance, 500 mL min^{-1} total flow rate, and $\text{GHSV} = 3 \times 10^5 \text{ h}^{-1}$. The concentrations of the outlet gases were real-time monitored by a Thermo Nicolet 380 FTIR spectrometer. All the turbings in the reactor system were heat-traced to 190 °C to prevent water condensation and ammonium nitrate deposition. The NO_x conversion (X), N_2 selectivity (S) and pseudo-first order rate constant (k) of NO_x reduction were calculated according to Eqs. (1)-(3), which were based on the data collected when the reaction substantially reached a steady state condition after about 30 min at each temperature. In Eq. (3), F and W were the total flow rate of the flow gas and sample mass, respectively [14].

$$X (\%) = \left(1 - \frac{[\text{NO}]_{\text{out}} + [\text{NO}_2]_{\text{out}}}{[\text{NO}]_{\text{in}}}\right) \times 100 \quad (1)$$

$$S (\%) = \left(1 - \frac{[\text{NO}_2]_{\text{out}} + 2 \times [\text{N}_2\text{O}]_{\text{out}}}{[\text{NH}_3]_{\text{in}} + [\text{NO}]_{\text{in}} - [\text{NH}_3]_{\text{out}} - [\text{NO}]_{\text{out}}}\right) \times 100 \quad (2)$$

$$k = -\frac{F}{W} \ln(1 - X) \quad (3)$$

Steady state kinetics experiments were conducted in a fixed bed quartz reactor every twenty degrees between 180 and 260 °C. Thus stable and low conversions of NO_x (< 20%) were achieved in an approximate kinetic regime. Over this temperature range, the NH_3 conversion was consistent with NO conversion for NbCZ with no outlet N_2O and NO_2 detected, suggesting NH_3 and NO oxidation is negligible. A much higher gas hourly space velocity ($1.2 \times 10^6 \text{ h}^{-1}$, with a total flow

rate of 2 L min⁻¹) and less than 200 mesh size powder catalyst were adopted to achieve kinetically controlled conditions and absence of external mass transport limitations. The typical reactant gas composition included 200-800 ppm NO, 200-800 ppm NH₃, 5% O₂, and N₂ in balance.

The rate of NO reduction as a function of reactant concentrations was expressed as a power-law rate in Eq. 4.

$$R_{\text{NO}} = k[\text{NO}]^{\alpha}[\text{NH}_3]^{\beta}[\text{O}_2]^{\gamma} \quad (4)$$

where, R_{NO} was the SCR rate, k was the apparent rate constant, and α , β , and γ were the reaction orders for NO, NH₃ and O₂, respectively.

2.3. Catalyst characterization

Temperature-programmed desorption of NO_x (NO_x-TPD) experiments were carried out in a fixed bed quartz reactor with the effluent gases monitored using a Thermo Nicolet 380 FTIR spectrometer. 100 mg powder catalyst was preheated in flowing 5% O₂/N₂ at 500 °C for 30 min to remove any possible impurities. After cooling down to 30 °C, the sample was exposed to a flow of 1000 ppm NO + 5% O₂ in N₂ for 60 min, followed by flushing with N₂ for 30 min to remove the physical-adsorbed molecules. Afterwards, the catalyst was heated up to 500 °C in 5% O₂/N₂ at a rate of 10 °C min⁻¹ for desorption of NO_x.

In situ DRIFT spectra were recorded by a Nicolet 6700 FTIR spectrometer equipped with a high-temperature environmental cell fitted with KBr window. The catalyst was finely ground and placed in a ceramic crucible and manually flattened. Prior to each experiment, the catalyst was pretreated at 500 °C in 10% O₂/N₂ with a total flow rate of 100 mL min⁻¹ for 30 min to remove traces of organic residues. Afterwards, background collection was performed after the sample was flushed by 100 mL min⁻¹ N₂ for 30 min at the corresponding temperature. For NH₃ adsorption, a feeding gas containing 1000 ppm NH₃ in N₂ with a total flow rate of 100 mL min⁻¹ passed through the sample for 60 min. After purging physisorbed NH₃ molecules by N₂ flow for 30 min, the DRIFT spectra of adsorbed species on catalysts were collected at the same temperature. NO+NH₃+O₂ co-adsorption were carried out through a similar procedure, in which 100 ml min⁻¹ feeding gas with 1000 ppm NO + 1000 ppm NH₃ + 10% O₂ in N₂ was introduced to the N₂-pretreated sample.

For the $\text{NO}+\text{O}_2$ reaction with pre-adsorbed NH_3 species over the catalyst, a similar procedure was performed for the pretreatment and the background collection steps. The catalysts were pre-adsorbed with 1000 ppm NH_3/N_2 for 60 min at 180 °C, followed by N_2 purging for 30 min to remove the weakly adsorbed NH_3 species. The 1000 ppm $\text{NO} + 10\% \text{O}_2$ in N_2 with a total flow rate of 100 ml min^{-1} was then introduced into the IR cell, and the spectra were recorded as a function of time. Similar procedures were carried out for the NH_3 and NH_3+NO reaction with pre-adsorbed N_xO_y species over the catalyst.

3. Results

3.1 SCR activity

Fig. 1 shows the SCR activities of CZ and NbCZ catalysts as a function of temperature. Without Nb modification, CZ shows poor activity within the whole temperature range (100-500 °C), with the maximum NO_x conversion less than 50% and even negative values at temperatures higher than 400 °C as a result of NH_3 over-oxidation to NO_x in Fig. 1a. The activity of NbCZ is greatly improved with above 80% NO_x conversion achieved at a wide temperature range from 200 to 450 °C. Furthermore, little N_2O or NO_2 is generated over NbCZ, accompanied by N_2 selectivity exceeding 95% within the whole temperature range. This indicates that the introduction of Nb species to CZ could suppress the unselective catalytic oxidation of NH_3 by O_2 to N_2O and NO_2 at high temperatures as shown in Fig. 1b. The presence of H_2O in the feeding gas reduces the catalytic activities at low temperatures (< 350 °C) but enhanced the activities at high temperatures (> 350 °C) for both the catalysts. The inhibition effect of water on the low-temperature SCR reaction is usually explained as an effect of a competitive between H_2O and NH_3/NO_x on the reaction sites [7]. The latter is usually explained as an inhibition effect of H_2O on the unselective catalytic oxidation of NH_3 [31], which also leads to increased N_2 selectivity at high temperatures. Fig 1c shows the k values of CZ and NbCZ at various temperatures, which are in similar trends with NO_x conversions in Fig. 1a.

3.2 Surface acidity

In order to determine the types of surface acid sites and their stability, DRIFT spectra of adsorbed ammonia species at different temperatures on CZ and NbCZ were collected in the range of 4000-2500 and 1800-900 cm^{-1} , and the results are shown in Fig. 2. The bands at 1150 and 1194 cm^{-1} are assigned to the symmetric bending vibration of NH_3 coordinated to Lewis acid sites [7, 13, 20], while those at 1418 and 1667 cm^{-1} are attributed to the asymmetric and symmetric bending vibrations of NH_4^+ bonded to Brønsted acid sites, respectively [7, 12, 13]. In the N-H stretching region, bands at 3390 and 3258 cm^{-1} are indicative of NH_3 adsorbed on Lewis acid sites [3, 12, 13]. The negative bands at 3768 and 3674 cm^{-1} are assigned to the O-H stretching in the surface hydroxyl groups [3, 7, 32]. It is worth noting that there are two types of Lewis acid sites on CZ, probably corresponding to the unsaturated Ce^{n+} and Zr^{n+} ions [8, 29], as indicated by two bands corresponding to symmetric bending vibrations of NH_3 at 1150 and 1194 cm^{-1} , respectively. Amide (NH_2) species (1550, 1300 and 1095 cm^{-1}) [3, 20, 33] deriving from the deprotonation of ammonia via partial oxidation are not stable at temperatures above 150 $^\circ\text{C}$.

Fig. 2b shows the DRIFT spectra of NH_3 adsorption on NbCZ. New bands at 3158, 3000 and 2750 cm^{-1} are attributed to NH_4^+ species bonded to Brønsted acid sites [12, 34, 35], while those at 1590 cm^{-1} and in the range of 1050-1250 cm^{-1} are assigned to NH_3 species coordinated to Lewis acid sites [3, 7, 20]. Clearly, the numbers of both Lewis and Brønsted acid sites increases on NbCZ as indicated by the stronger bands compared with those on CZ. Considering the decrease in the surface coverage of $\text{Ce}^{n+}/\text{Zr}^{n+}$ after niobia loading, these additional Lewis acid sites should derive from the formation of unsaturated Nb^{n+} cations. According to our previous study [14], the additional Brønsted acid sites results mainly from Nb-OH bonds, which is formed by combination of surface H_2O and Nb=O bond as indicated by the bands at 973-991 cm^{-1} [13, 36]. Different from CZ, the bands of $\text{NH}_3/\text{NH}_4^+$ and NH_2 (at 1560 and 1295-1330 cm^{-1}) species on NbCZ can be observed at the temperature as high as 350 $^\circ\text{C}$, indicating more NH_3 or NH_2 like-species available at high temperatures. NH_2 is important for the high-temperature SCR reaction as an intermediate in the “E-R” route [3, 20, 31, 35].

Fig. 3 shows the Lewis and Brønsted acidities, which were obtained by calculating the integrated areas of bands at 1095-1212 and 1418-1430 cm^{-1} in the DRIFT spectra in Fig. 2, respectively. The data of IR intensity were normalized by the catalyst surface areas (102 and 74

$\text{m}^2 \text{g}^{-1}$ for CZ and NbCZ, respectively). Both the amounts of Lewis and Brønsted acid sites follow the order of NbCZ > CZ, demonstrating the contribution of niobia to the total surface acidity. It is noted that Lewis acid sites on NbCZ appear to be more strongly coordinated to NH_3 at the temperatures higher than 350 °C. Due to its stronger interaction with ammonia than Ce^{n+} or Zr^{n+} cations, the unsaturated Nb^{n+} cations in the surface NbO_x species could increase the thermal stability of adsorbed ammonia on NbCZ.

Fig. 4 shows the TPD profiles of NO_x (NO_2 and NO) for CZ and NbCZ catalysts in the temperature range 30-500 °C. Both the catalysts show several obvious NO_x desorption peaks in low (50-110 °C) and high (250-450 °C) temperature ranges, corresponding to the desorption of weakly adsorbed N_xO_y (NO^- or NO_2^-) species and decomposition of NO_3^- (nitrates), respectively [32, 37, 38]. The total amounts of desorbed NO_x were estimated from these profiles and the values are 1.92 and 1.00 $\mu\text{mol m}^{-2}$ for CZ and NbCZ, respectively, indicating the inhibition effect of Nb species on the NO_x adsorption. The NO desorption peak centered at 420 °C on CZ is mainly produced by the thermodynamic balance of NO_2 - NO cycle from the NO_2 derived from decomposition of nitrates [37], and hereby should be ascribed to NO_2 when calculating the NO_2/NO_x (NO_2+NO) ratio. In this way, the calculated NO_2/NO_x ratios are 99% and 93% for NbCZ and CZ, respectively, indicating that more NO_2 than NO like-species desorbs from the former catalyst. This illustrates that almost all the NO_x adsorbed species over NbCZ are nitrates. Furthermore, the NO_2 desorption peak shifts to lower temperature for NbCZ, suggesting the reduced thermal stability of nitrates after niobia loading. These probably result from the abundant active oxygen species at the Nb^{n+} - O^{2-} - Ce^{n+} interface and the acidic nature of surface NbO_x species, as discussed in our previous study [14]. It has been reported the unstable nitrates would readily participate in a “L-H” reaction route as the reactants, while the stable nitrates could potentially deactivate the ceria based catalysts by blocking the interaction of Ce^{n+} active sites with NH_3 [3, 20, 25, 39]. In this sense, the less stable nitrates on NbCZ are more favorable to NH_3 -SCR reaction than those stable ones on CZ.

3.3 DRIFTS studies

3.3.1. Reaction between NO_x and ad- NH_3 species

The DRIFT spectra of CZ and NbCZ catalysts with the pre-adsorbed NH_3 upon exposing in $\text{NO}+\text{O}_2$ at $180\text{ }^\circ\text{C}$ as a function of time are shown in Fig. 5. Generally, the amount of the NH_3 species adsorbed on the catalysts decreases upon exposing in $\text{NO}+\text{O}_2$, indicating their consumption by reacting with gaseous NO_x /surface N_xO_y species. After pre-adsorption of ammonia, NH_3 species coordinated to Lewis acid sites (1148 , 1198 , 3275 and 3380 cm^{-1}) and a few NH_4^+ species bonded to Brønsted acid sites (1433 cm^{-1}) are present on the surface of CZ. Bands assigned to N_xO_y species such as bridging nitrates (1606 and 1157) [3, 40], bidentate nitrates (1012 , 1550 and 1579 cm^{-1}) [20, 40], monodentate nitrates (1527 and 1246 cm^{-1}) [20, 32, 40] nitrates, NO^- (1184 cm^{-1}) [10, 40], NO_2^- (1494 cm^{-1}) [40] and *trans*- $\text{N}_2\text{O}_2^{2-}$ (1403 cm^{-1}) species [4, 40] are readily evident after introduction of $\text{NO}+\text{O}_2$ for 1 min. These bands increase in intensity gradually with time, potentially due to the basic nature of ceria. It is worth noting that NH_3 species coordinated to Lewis acid sites (3275 and 3380 cm^{-1}) resides even after 30 min, suggesting a slow consumption of NH_3 species by N_xO_y species or gaseous NO_x over CZ.

The bands of NH_3 -derived species, i.e. coordinated NH_3 (1196 , 1597 , 3242 and 3358 cm^{-1}), NH_4^+ (1420 and 1665 cm^{-1}) and amide species (1326 cm^{-1}), are much more pronounced on NbCZ catalyst. When the catalyst is purged with $\text{NO}+\text{O}_2$ for just 3 min, all the bands ascribed to ammonia ad-species diminish, accompanied by the strengthened bands corresponding to N_xO_y species. This means that niobia loading can accelerate the reaction between surface N_xO_y /gaseous NO_x and ad- NH_3 species. Moreover, the nitrates related bands are obviously lower in intensity on this catalyst after exposing in $\text{NO}+\text{O}_2$ for 30 min, confirming again that surface sites are less saturated by N_xO_y species after niobia loading.

3.3.2. Reaction between NH_3 and ad- N_xO_y species

The DRIFT spectra of catalysts with the pre-adsorbed N_xO_y species upon exposing in NH_3 at $180\text{ }^\circ\text{C}$ as a function of time are shown in Fig. 6. After pre-adsorption in $\text{NO}+\text{O}_2$, the surface of the catalysts are covered by bridging nitrates (1606 - 1613 and 1157 - 1160 cm^{-1}), bidentate nitrates (1009 - 1012 , 1543 - 1556 and 1572 cm^{-1}) and monodentate nitrates (1524 - 1538 and 1236 - 1252 cm^{-1}). Additional bands at 1033 cm^{-1} on CZ can be assigned to *cis*- $\text{N}_2\text{O}_2^{2-}$ species [4, 40]. CZ and NbCZ show similar variations of the DRIFT spectra after introduction of NH_3 . Unlike the case of

pre-adsorbed NH_3 in Fig. 5, most of the pre-adsorbed N_xO_y species are stable on the catalysts even after the introduction of NH_3 for 30 min, and the bands of NH_3 -associated species are not observed within the first 5 min. These indicate that it is quite difficult for NH_3 to be adsorbed on the NO_x -pre-adsorbed catalyst, and the reaction between ad- NH_3 and ad- N_xO_y species is probably limited by strong N_xO_y coverage. Nevertheless, it is seen that the bands ascribed to NH_4^+ on Brønsted acid sites (1430 and 1665 cm^{-1}) and those to NH_3 coordinated to Lewis acid sites (3379 and 3247 cm^{-1}) are significantly stronger on NbCZ than those on CZ (1430, 3363 and 3264 cm^{-1}) after 30 min. This fact verifies again that the introduction of niobia could increase the number of acid sites and induce NH_3 and NO_x to be adsorbed on $\text{Nb}^{n+}/\text{Nb-OH}$ and Ce^{n+} sites separately, which can compensate for the side effect of competitive adsorption of NH_3 and N_xO_y on Ce^{n+} sites.

3.3.3. Reaction between $\text{NO}+\text{NH}_3$ and ad- N_xO_y species

It is worth studying for co-introducing NO and NH_3 on the N_xO_y pre-adsorbed catalysts since there are always these two gaseous reactants in SCR reaction. As shown in Fig. 7, the nitrate related bands including bridging nitrates (1606-1613 and 1157-1160 cm^{-1}), bidentate nitrates (1012-1014, 1543-1556 and 1572 cm^{-1}) and monodentate nitrates (1524-1538 and 1235-1252 cm^{-1}), as well as NH_4^+ on Brønsted acid sites (1430 and 1665 cm^{-1}) and NH_3 coordinated to Lewis acid sites (3363-3379 and 3247-3264 cm^{-1}), are observed in the spectra. NH_4NO_3 species with bands at 1360 and 1380 cm^{-1} [4, 41, 42] is formed on CZ after 3 min in Fig. 7a, which is not observed in the case of passing NH_3 over CZ with pre-adsorbed N_xO_y (Fig. 6a). These bands, as well as those nitrate related ones, always exist with time. It indicates that the formation of NH_4NO_3 requires co-feeding gaseous NO and NH_3 , and it as an intermediate cannot react further and accumulate on CZ.

Interestingly, the intensities of NH_4NO_3 related bands reach the maximum immediately on NCZ after co-introduction of NO and NH_3 and then decrease with time. Meanwhile, the intensities of the nitrate related bands decline much more quickly on this catalyst. These indicate that in the presence of gaseous NH_3 and NO , niobia loading facilitates the reaction between surface N_xO_y species and ads- NH_3 species and accelerates the decomposition of NH_4NO_3 . Therefore, it is plausible to suggest that the SCR reaction over NbCZ catalyst at 180 °C may occur via the

combination of surface N_xO_y and ads- NH_3 species to NH_4NO_3 and its further decomposition to H_2O and N_2 .

3.3.4 NH_3+NO+O_2 co-adsorption

To identify surface species presented on catalyst under reaction conditions, the DRIFT spectra of CZ and NbCZ following contact with NH_3+NO+O_2 at various temperatures are shown in Fig. 8. NO^- species (1180 cm^{-1}), bridging nitrates (1604 and 1213 cm^{-1}), bidentate nitrates (1554 , 1576 and 1008 cm^{-1}), monodentate nitrates (1529 and 1237 cm^{-1}) and *cis*- $N_2O_2^{2-}$ (1026 cm^{-1}) are present on CZ. The bands attributed to coordinated NH_3 to Lewis acid sites (3380 and 3275 cm^{-1}) are also detected. The oxidation of weakly adsorbed NO^- species (1180 cm^{-1}) to more stable nitrates is observed at 150 - $250\text{ }^\circ\text{C}$. The NO related band (1690 cm^{-1}) appears at temperatures no less than $250\text{ }^\circ\text{C}$. With the temperature increasing, the NH_3 related bands diminishes and the nitrate related bands increase in intensity, indicating that the surface of CZ is dominantly covered with nitrates especially at high temperatures. It is difficult for ammonia to be adsorbed on the surface strongly covered with nitrates. The formation of NH_4NO_3 (1380 and 1360 cm^{-1}) can be observed in the temperature range 200 - $350\text{ }^\circ\text{C}$. This species disappear at high temperatures, which may be caused by the competitive oxidation of ammonia in the presence of oxygen.

For NbCZ catalyst, bridging nitrates (1606 and 1210 cm^{-1}), bidentate nitrates (1565 and 1015 cm^{-1}) and monodentate nitrates (1531 and 1237 cm^{-1}) are observed in Fig. 8b. Compared with CZ, NO^- species is absent on NbCZ. Instead, nitrates turn to be the main N_xO_y species even at a temperature as low as $150\text{ }^\circ\text{C}$, which should be due to facile oxidation of adsorbed NO^- to nitrates. Again, the bands associated with nitrates decrease in intensity more rapidly with temperature, indicating that the thermal stability of nitrates is greatly weakened by niobia addition. These correlate well with the NO_x -TPD results in Fig. 4. NH_4NO_3 species (1380 and 1360 cm^{-1}), an intermediate from the reaction between surface ads- NH_3 and nitrates species, appears in the temperature range 150 - $300\text{ }^\circ\text{C}$. This confirms again that the “L-H” mechanism is the main reaction route over NbCZ at low temperatures ($< 300\text{ }^\circ\text{C}$). Compared with CZ, the NH_3 derived bands disappear on NbCZ. Considering the stronger acidity of NbCZ and less inhibition effect of nitrates on NH_3 adsorption (as shown in Figs. 6 and 7), this abnormal phenomenon is probably

caused by the accelerated SCR reaction which consumes most of the surface adsorbed NH_3 on NbCZ.

3.4 Kinetic studies

To determine the reaction orders with respect to NO and NH_3 over NbCZ at various temperatures, the concentration of NO/ NH_3 was varied from 200 to 800 ppm with another reactant (NH_3/NO) and O_2 kept at 500 ppm and 5%, respectively. Regression analysis of the experimental data was performed to calculate the reaction orders with confidence intervals of 99%, and the results are listed in Table 1. The rates of NO reduction as a function of the inlet NO and NH_3 concentrations at 180-260 °C are shown in Fig. 9.

As shown in Fig. 9a, the rates of NO reduction at different temperatures are found to increase linearly with NO concentration. The reaction order for NO (α) is between 0 and 1, which is explained by the fact that NO can participate in SCR reaction in the form of both gaseous and surface adsorbed N_xO_y species [43]. Therefore, SCR reaction may follow both “E-R” and “L-H” mechanisms over NbCZ catalyst. It is interesting to note that the reaction rate at 180 °C almost keeps steady when NO concentration increases from 200 to 800 ppm. The reaction order for NO concentration ($\alpha=0.365$) is close to zeroth-order, indicating that NO involves in SCR reaction mainly as adsorbed species at low temperatures according to “L-H” mechanism. At the temperatures higher than 180 °C, the value of α is more close to 1, suggesting that gaseous NO plays a more critical role in the reaction, which is possibly associated with the more unstable nature of nitrates species. In this case, “E-R” mechanism accordingly becomes the dominating reaction route on NbCZ at high temperatures.

It is noted in Fig. 9b that NO reduction rate decreases slightly with increasing NH_3 concentration in the presence of 5% O_2 at 180 and 200 °C. The reaction orders (β) with respect to NH_3 are found to be -0.177 and -0.096. These values are close to zeroth-order for NH_3 , suggesting that NH_3 needs to be initially adsorbed on the catalyst in order to react with surface N_xO_y /gaseous NO_x . Interestingly, the correlations between NO reduction rate and NH_3 concentration at 220-260 °C show diverse features in the low and high NH_3 concentration ranges. The absolute value of β_1 increases from 0.172 to 0.366, whereas that of β_2 decreases from -0.140 to -0.057. A similar case has been reported by Orlink on a $\text{V}_2\text{O}_5/\text{TiO}_2$ catalyst [44]. It is usually explained by

that a side NH_3 -oxidation reaction besides the NH_3 -SCR reaction accounts for the decreased apparent NO reduction rate at high NH_3 concentrations [45-47]. However, in this study, NH_3 oxidation is negligible at 180-260 °C (not shown) [14]. Therefore, the inhibition effect of excessive NH_3 on NO reduction rate results probably from the competitive adsorption of NH_3 and NO, in which the adsorptive sites for N_xO_y species may be blocked by surface NH_3 species. This speculation is supported by the fact that the absolute value of β (180-200 °C) or β_2 (220-260 °C) decreases with temperature, as the “E-R” reaction route is more dominant at high temperatures and surface N_xO_y species plays a less important role.

4. Discussion

As shown in Fig. 1, the SCR activity of CZ is quite poor at 180 °C, while about 80 % NO_x conversion is achieved over NbCZ. At this temperature, more NH_3 is adsorbed on NbCZ as shown in Fig. 3, indicating a stronger NH_3 adsorption capacity derived from niobia loading. Based on the DRIFTS studies, Ce^{n+} sites are the main sites for both NH_3 and NO adsorption on CZ (Eqs. 5 and 6), while NO and NH_3 are preferentially adsorbed on Ce^{n+} and Nb-OH/Nb $^{n+}$ sites of NbCZ (Eqs. 6-8), respectively. All the NH_3 related bands diminish quickly when passing $\text{NO}+\text{O}_2$ over NbCZ with pre-adsorbed NH_3 (Fig. 5b). Some nitrates species are also removed by purging NH_3+NO over this modified catalyst (Fig. 7b). In the $\text{NH}_3+\text{NO}+\text{O}_2$ co-adsorption experiment (Fig. 8), both the NH_3 and NO derived species are observed and evolve with temperature, indicating the co-adsorption and reaction of the two reactants. These results suggest that both adsorbed NH_3 and N_xO_y species could participate as important intermediates in the SCR reaction over NbCZ, which is further verified by the approximate zeroth-orders for NH_3 and NO at 180 °C in the kinetic study (Fig. 9). Thus, both adsorptions of NH_3 and NO_x are important intermediate processes in SCR reaction and the reaction over NbCZ at low temperatures is believed mainly to follow an “L-H” route.

As shown in Figs. 7 and 8, NH_4NO_3 formed by the reaction between ads- NH_3 and N_xO_y species is a critical intermediate species in this “L-H” reaction route (Eq. 9). Fig. 10 shows the evolutions of the band annotated as bidentate nitrate estimated from Figs. 6 and 7 as a function of

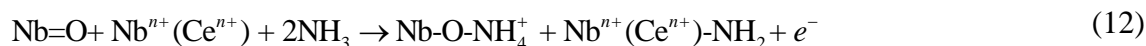
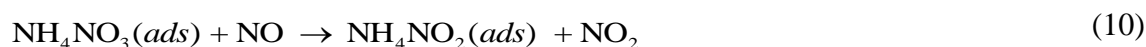
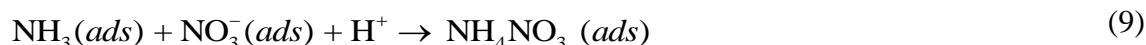
reaction time. It keep almost unchanged on CZ in the presence and absence of gaseous NO, while different trends are observed on the modified catalyst. Combined with high SCR activity of NbCZ, it implies that the presence of NO is a necessary condition for reactions between ads-NH₃ and N_xO_y species. It is clear that Nb loading accelerates the reaction between ads-NH₃ and N_xO_y species as indicated by the fast formation of NH₄NO₃ within the first 1 min, while it takes about 5 min for the NH₄NO₃ related band to reach the maximum intensity on CZ. As the reaction continues, NH₄NO₃ species accumulates on CZ, while it is consumed quickly on NbCZ, indicating the promoted decomposition of ammonium nitrates by the addition of niobia to the catalyst. It has been reported that the direct decomposition of NH₄NO₃ would produce N₂O [48], which is not detected at the temperatures below 300 °C over NbCZ in this study (Fig. 1b). According to the literatures [25, 32, 39, 41, 48-50], NH₄NO₃ does not behave as a terminal product in a stream containing NO and is suggested to be efficiently reduced to NH₄NO₂ (Eq. 10), from which N₂ and H₂O are swiftly produced (Eq. 11). Hence, the reduction of NH₄NO₃ to NH₄NO₂ by NO and the simultaneous feasible decomposition of NH₄NO₂ are considered as the important steps of the “L-H” reaction route for NbCZ catalyst at low temperatures. Similar mechanisms have been also reported for some Ce [4, 25] and Mn catalysts [32, 51].

On the other hand, it is noticeable in Figs. 4 and 8b that the adsorbed nitrates species are unstable and their thermal stability is significantly weakened by niobia loading. In this case, the SCR reaction on NbCZ at high temperatures (> 350 °C) is suggested to follow an “E-R” mechanism. The increased reaction order (α) for NO (Table 1) also indicates that gaseous NO behaves a more crucial role in the NH₃-SCR reaction route at high temperatures. It is concluded by a lot of researchers [3, 4, 8, 16, 20] that this “E-R” mechanism involves the formation of amide (NH₂) species via deprotonation of NH₃, and the subsequent reaction between NH₂ and gaseous NO to generate N₂ and H₂O. In our study, it is found that both the coordinated NH₃ to Lewis acid sites and NH₄⁺ to Brønsted acid sites can participate the SCR reaction, in agreement with the literatures [7, 8, 20]. However, it should also be addressed that the stable nitrates on CZ could occupy the surface active sites and prohibit the competitive adsorption of NH₃ as shown in Fig. 8a. A similar inhibition effect by NO adsorption has been proposed by researches on catalysts such as WO_x-CeO₂/TiO₂ [3], MoO_x-CeO₂ [20] and ZP/CZ [25].

According to the above discussion, the NH_3 -SCR reaction mechanism over NbCZ catalyst can be proposed as “L-H” and “E-R” mechanisms at low and high temperatures, respectively, and the tentative mechanisms are presented in Fig. 11. The introduction of niobia to CZ can increase the NH_3 -SCR activity significantly at both low and high temperatures. The promotion effects of niobia on the low-temperature activity include the following aspects. Firstly, it is proposed in Figs. 4 and 8b that the N_xO_y species on NbCZ is mainly nitrates, while large amount of NO^- or $\text{N}_2\text{O}_2^{2-}$ species are present on CZ. This indicates that the introduction of niobia facilitates the oxidation of NO-like (NO^- and N_2O_2) species on Ce^{n+} sites to nitrates, which can be ascribed to the better reducibility derived from the Nb^{n+} - Ce^{n+} interaction that induces the generation of more Ce^{3+} cations and weakly bonded oxygen species [12,13]. According to the XPS measurements in our previous work [14], the surface atomic ratios of Ce^{3+}/Ce are 18% and 39% of CZ and NbCZ, and the relative ratios of weakly bonded oxygen $\text{O}\alpha/\text{O}$ are 9% and 17%, respectively. Meanwhile, the weak bonding of NO_2 -like species on NbCZ at relatively low temperatures may also enhance the activity by facilitating the “fast SCR” reaction. Secondly, the introduced abundant Nb^{n+} and Nb-OH sites as acid sites increase the surface acidity of the catalyst, making ammonia and NO_x adsorbed on $\text{Nb}^{n+}/\text{Nb-OH}$ and Ce^{n+} sites separately rather than their competitive adsorption on Ce^{n+} sites. This weakens the inhibition effect on NH_3 adsorption by stable nitrates and promotes the occurrence of the SCR reaction. Finally, it has been reported that solid acids can catalyze both the reaction of NH_4NO_3 to NH_4NO_2 [48, 52] and the further decomposition process of NH_4NO_2 [39, 50] at significantly low temperatures ($< 100\text{ }^\circ\text{C}$). However, if the accumulated NH_4NO_3 could not be efficiently reduced by NO at $180\text{ }^\circ\text{C}$, it may deactivate the catalyst by blocking the “L-H” reaction route [48]. Accordingly, the reaction of ads- NH_3 with nitrates species, the reduction of NH_4NO_3 to NH_4NO_2 species and the further decomposition of NH_4NO_2 species are all accelerated on NbCZ catalyst as indicated in Fig. 10, resulting in a superior low-temperature activity.

At high temperatures, the stable nitrates on CZ occupy Ce^{n+} active sites and inhibit the adsorption of NH_3 . This, as well as the competitive oxidation of NH_3 , leading to negative conversion of NO_x . Contrarily, the unstable nitrates on NbCZ could provide more Ce^{n+} sites available for NH_3 adsorption. More importantly, the abundant Nb=O bonds in surface NbO_x species could also promote the activation of NH_3 to NH_2 as shown in Fig. 2b (Eq. 12). In this way,

as confirmed by the kinetic study (Fig. 9), activated NH_2 species readily reacts with gaseous NO_x , resulting in promoted high-temperature activity of NbCZ catalyst (Eq. 13).



5. Conclusions

$\text{NbO}_x/\text{Ce}_{0.75}\text{Zr}_{0.25}\text{O}_2$ catalyst exhibits above 80% NO_x conversion and above 95% N_2 selectivity in the temperature range from 200 to 450 °C. Based on the *in situ* DRIFTS and kinetic studies, it is proposed that both a “ $\text{NH}_4^+\text{+NO}_3^-$ ” reaction route at low temperatures and a “ $\text{NH}_2\text{+NO}$ ” reaction route at high temperatures can be accelerated by niobia loading. The enhanced acidity by niobia addition can accelerate the reaction between ads- NH_3 and nitrates species to form NH_4NO_3 , the reduction of NH_4NO_3 by NO and the further catalytic decomposition of NH_4NO_2 to N_2 and H_2O at low temperatures. At higher temperatures, more stable acid sites arising from niobia enhance the ammonia adsorption capacity and decrease the stability of nitrates species, contributing to the reaction of activated NH_2 species with gaseous NO .

Acknowledgements

The authors would like to acknowledge the financial support from projects of the National Natural Science Foundation of China (Nos. 51202126 and 51372137) and the Ministry of Science

and Technology, PR China for financial support from Project 2015AA034603.

This work has been partly performed within the Competence Centre for Catalysis (KCK) at Chalmers University of Technology. KCK is financially supported by Chalmers University of Technology and financially supported by the Swedish Energy Agency and the member companies: AB Volvo, ECAPS AB, Haldor Topsøe A/S, Scania CV AB, Volvo Car Corporation AB and Wärtsilä Finland Oy.

References

- [1] P. Forzatti, *Appl. Catal. A: Gen.* 222 (2001) 221-236.
- [2] G. Busca, L. Lietti, G. Ramis, F. Berti, *Appl. Catal. B: Environ.* 18 (1998) 1-36.
- [3] L. Chen, J.H. Li, M.F. Ge, *Environ. Sci. Technol.* 44 (2010) 9590-9596.
- [4] L. Chen, J.H. Li, M.F. Ge, L. Ma, H.Z. Chang, *Chinese J. Catal.* 32 (2011) 836-841.
- [5] W.P. Shan, F.D. Liu, H. He, X.Y. Shi, C.B. Zhang, *Chem. Commun.* 47 (2011) 8046-8048.
- [6] L. Chen, D. Weng, Z.C. Si, X.D. Wu, *Prog. Nat. Sci-Mater.* 22 (2012) 265-272.
- [7] W.P. Shan, F.D. Liu, H. He, X.Y. Shi, C.B. Zhang, *Appl. Catal. B: Environ.* 115-116 (2012) 100-106.
- [8] Y. Peng, K.Z. Li, J.H. Li, *Appl. Catal. B: Environ.* 140-141 (2013) 483-492.
- [9] Z.R. Ma, X.D. Wu, Y. Feng, Z.C. Si, D. Weng, *Catal. Commun.* 69 (2015) 188-192.
- [10] M. Casapu, O. Kröcher, M. Mehring, M. Nachtegaal, C. Borca, M. Harfouche, D. Grolimund, *J. Phys. Chem. C* 114 (2010) 9791-9801.
- [11] M. Casapu, A. Bernhard, D. Peitz, M. Mehring, M. Elsener, O. Kröcher, *Appl. Catal. B: Environ.* 103 (2011) 79-84.
- [12] Z.R. Ma, D. Weng, X.D. Wu, Z.C. Si, B. Wang, *Catal. Commun.* 27 (2012) 97-100.
- [13] R.Y. Qu, X. Gao, K.F. Cen, J.H. Li, *Appl. Catal. B: Environ.* 142-143 (2013) 290-297.
- [14] Z.R. Ma, X.D. Wu, Z.C. Si, D. Weng, J. Ma, T.F. Xu, *Appl. Catal. B: Environ.* 179 (2015) 380-394.
- [15] R.Y. Qu, Y. Peng, X.X. Sun, J.H. Li, X. Gao, K.F. Cen, *Catal. Sci. Technol.* 6 (2016) 2136-2142.
- [16] J. Zhu, F. Gao, L.H. Dong, W.J. Yu, L. Qi, Z. Wang, L. Dong, Y. Chen, *Appl. Catal. B: Environ.* 95 (2010) 144-152.
- [17] H.Z. Chang, M.T. Jong, C.Z. Wang, R.Y. Qu, Y. Du, J.H. Li, J.M. Hao, *Environ. Sci. Technol.* 47 (2013) 11692-11699.
- [18] X.L. Li, Y.H. Li, *J. Mol. Catal. A: Chem.* 386 (2014) 69-77.
- [19] X.L. Li, Y.H. Li, *Reac. Kinet. Mech. Cat.* 112 (2014) 27-36.
- [20] Z.M. Liu, S.X. Zhang, J.H. Li, L.L. Ma, *Appl. Catal. B: Environ.* 144 (2014) 90-95.
- [21] J.H. Wang, X.S. Dong, Y.J. Wang, Y.D. Li, *Catal. Today* 245 (2015) 10-15.
- [22] S.P. Ding, F.D. Liu, X.Y. Shi, K. Liu, Z.H. Lian, L.J. Xie, H. He, *ACS Appl. Mater. Interfaces* 7 (2015) 9497-9506.
- [23] Z.C. Si, D. Weng, X.D. Wu, R. Ran, Z.R. Ma, *Catal. Commun.* 17 (2012) 146-149.
- [24] F. Li, Y.B. Zhang, D.H. Xiao, D.Q. Wang, X.Q. Pan, X.G. Yang, *ChemCatChem* 2 (2010) 1416-1419.
- [25] J. Yu, Z.C. Si, L. Chen, X.D. Wu, D. Weng, *Appl. Catal. B: Environ.* 163 (2015) 223-232.
- [26] J. Yu, Z.C. Si, M. Zhu, X.D. Wu, L. Chen, D. Weng, J.S. Zou, *RSC Adv.* 5 (2015) 83594-83599.
- [27] T.T. Gu, Y. Liu, X.L. Weng, H.Q. Wang, Z.B. Wu, *Catal. Commun.* 12 (2010) 310-313.
- [28] Z.C. Si, D. Weng, X.D. Wu, J. Yang, B. Wang, *Catal. Commun.* 11 (2010) 1045-1048.
- [29] Z.C. Si, D. Weng, X.D. Wu, Z.R. Ma, J. Ma, R. Ran, *Catal. Today* 201 (2013) 122-130.
- [30] H.Z. Chang, L. Ma, S.J. Yang, J.H. Li, L. Chen, W. Wang, J.M. Hao, *J. Hazard. Mater.* 262 (2013) 782-788.
- [31] L. Lietti, I. Nova, P. Forzatti, *Top. Catal.* 11 (2000) 111-122.

- [32] T.T. Gu, R.B. Jin, Y. Liu, H.F. Liu, X.L. Weng, Z.B. Wu, *Appl. Catal. B: Environ.* 129 (2013) 30-38.
- [33] J.M.G. Amores, V.S. Escibano, G. Ramis, G. Busca, *Appl. Catal. B: Environ.* 13 (1997) 45-58.
- [34] M.A. Centeno, I. Carrizosa, J.A. Odriozola, *J. Alloy. Compd.* 323 (2001) 597-600.
- [35] D.K. Sun, Q.Y. Liu, Z.Y. Liu, G.Q. Gui, Z.G. Huang, *Appl. Catal. B: Environ.* 92 (2009) 462-467.
- [36] L.J. Burcham, J. Datka, I.E. Wachs, *J. Phys. Chem. B* 103 (1999) 6015-6024.
- [37] B. Azambre, I. Atribak, A. Bueno-López, A. García-García, *J. Phys. Chem. C* 114 (2010) 13300-13312.
- [38] X.D. Wu, F. Lin, H.B. Xu, D. Weng, *Appl. Catal. B: Environ.* 96 (2010) 101-109.
- [39] M. Li, Y. Yeom, E. Weitz, W.M.H. Sachtler, *Catal. Lett.* 112 (2006) 129-132.
- [40] K.I. Hadjiivanov, *Catal. Rev.* 42 (2000) 71-144.
- [41] I. Nova, C. Ciardelli, E. Tronconi, D. Chatterjee, B. Bandl-Konrad, *Catal. Today* 114 (2006) 3-12.
- [42] F.A. Miller, C.H. Wilkins, *Anal. Chem.* 24 (1952) 1253-1294.
- [43] M.F. Fu, C.T. Li, P. Lu, L. Qu, M.Y. Zhang, Y. Zhou, M. Yu, Y. Fang, *Catal. Sci. Technol.* 4 (2014) 14-25.
- [44] S.N. Orlik, V.A. Ostapyuk, M.G. Martsenyuk-Kukharuk, *Kinet. Catal.* 36 (1995) 284-289.
- [45] H.Y. Huang, R.Q. Long, R.T. Yang, *Appl. Catal. A: Gen.* 235 (2002) 241-251.
- [46] G.S. Qi, R.T. Yang, *J. Catal.* 217 (2003) 434-441.
- [47] P.S. Metkar, N. Salazar, R. Muncrief, V. Balakotaiah, M.P. Harold, *Appl. Catal. B: Environ.* 104 (2011) 110-126.
- [48] A. Savara, M.-J. Li, W.M.H. Sachtler, E. Weitz, *Appl. Catal. B: Environ.* 81 (2008) 251-257.
- [49] A. Grossale, I. Nova, E. Tronconi, D. Chatterjee, M. Weibel, *J. Catal.* 256 (2008) 312-322.
- [50] M. Li, J. Henao, Y. Yeom, E. Weitz, W.M.H. Sachtler, *Catal. Lett.* 98 (2004) 5-9.
- [51] Z.H. Lian, F.D. Liu, H. He, X.Y. Shi, J.S. Mo, Z.B. Wu, *Chem. Eng. J.* 250 (2014) 390-398.
- [52] Y.H. Yeom, J. Henao, M.J. Li, W.M.H. Sachtler, E. Weitz, *J. Catal.* 231 (2005) 181-193.

Table captions

Table 1 Reaction orders for NO and NH₃ concentrations over NbCZ at various temperatures.

Figure captions

Fig. 1. (a) NO_x conversions, (b) N₂ selectivities and (c) *k* values of the catalysts for NH₃-SCR reaction. Catalysts: (1) CZ, (2) NbCZ, (3) CZ with 5% H₂O, and (4) NbCZ with 5% H₂O. Reaction conditions: 500 ppm NH₃, 500 ppm NO, 5% O₂, 12% CO₂ and N₂ in balanced.

Fig. 2. DRIFT spectra of adsorbed species on (a) CZ and (b) NbCZ arising from contact with NH₃+N₂ at different temperatures.

Fig. 3. The integrated area for bands of NH₃ adsorbed on (a) Lewis and (b) Brønsted acid sites over the CZ and NbCZ per catalyst surface area as a function of temperature.

Fig. 4. TPD profiles of NO and NO₂ over (1) CZ and (2) NbCZ catalysts.

Fig. 5. DRIFT spectra at 180 °C upon passing NO+O₂ over the (a) CZ and (b) NbCZ catalysts with pre-adsorbed NH₃ species.

Fig. 6. DRIFT spectra at 180 °C upon passing NH₃ over the (a) CZ and (b) NbCZ catalysts with pre-adsorbed N_xO_y species.

Fig. 7. DRIFT spectra at 180 °C upon passing NH₃+NO over the (a) CZ and (b) NbCZ catalysts with pre-adsorbed N_xO_y species.

Fig. 8. DRIFT spectra of adsorbed species on the (a) CZ and (b) NbCZ arising from contact with NO+NH₃+O₂ at different temperatures.

Fig. 9. Dependence of NO reduction rate on (a) NO and (b) NH₃ concentrations over NbCZ catalyst at 180-260 °C.

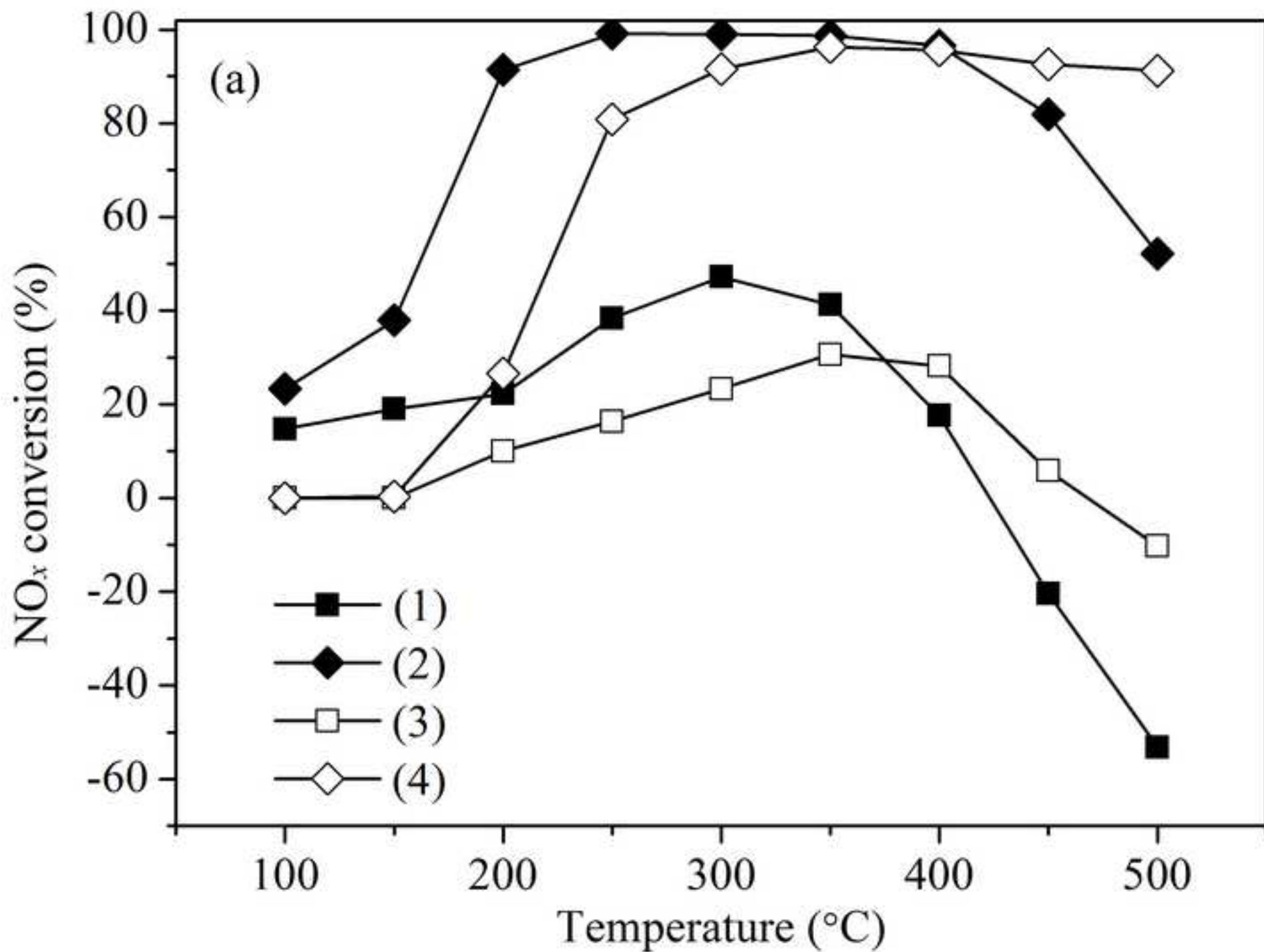
Fig. 10. Variations of intensity of bidentate nitrate related band (1543-1556 cm⁻¹) obtained from Figs. 6 and 7 and those of NH₃NO₄ related band (1360 cm⁻¹) from Fig. 7 as a function of reaction time over (a) CZ and (b) NbCZ at 180 °C.

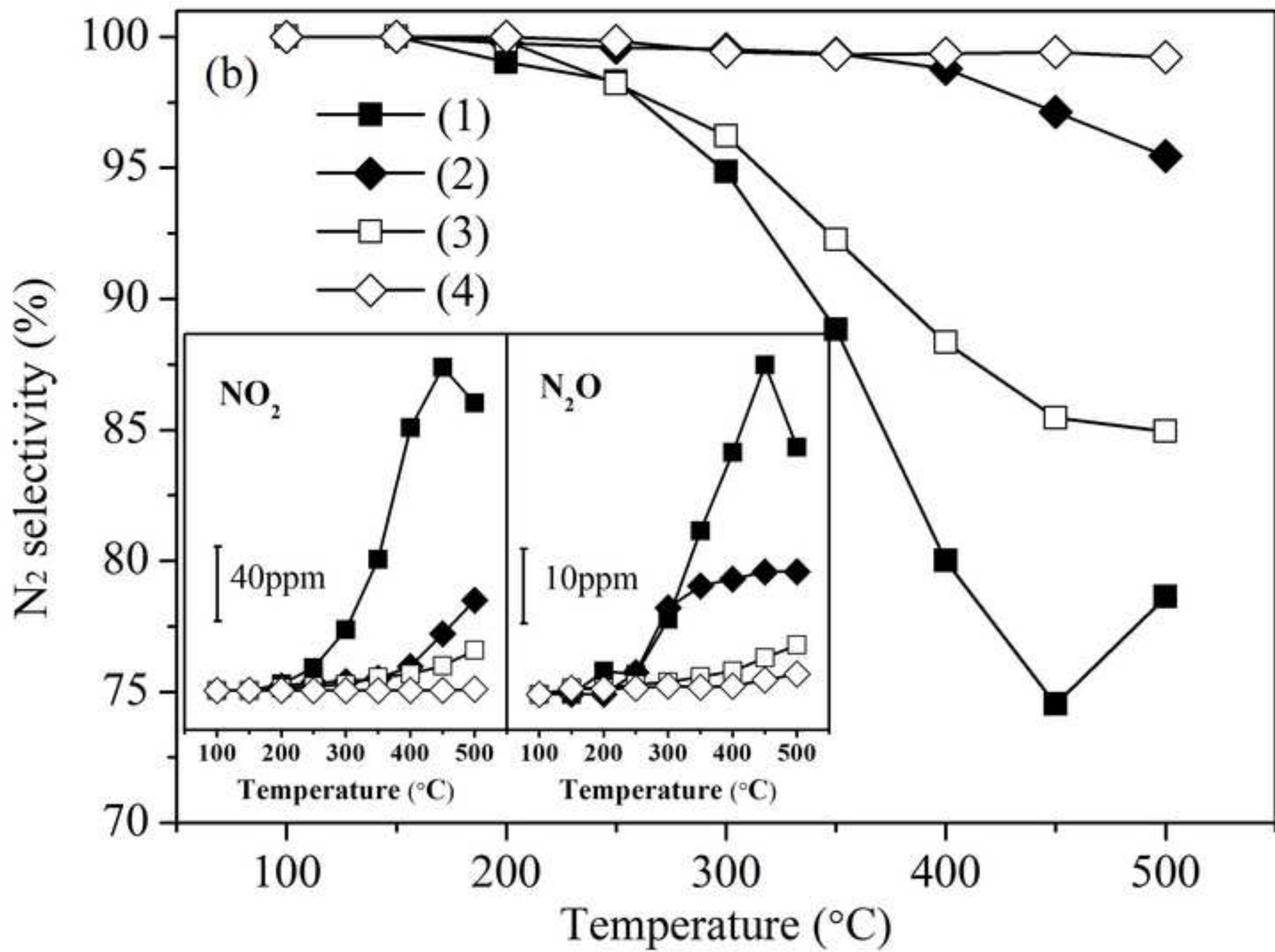
Fig. 11. The tentative NH₃-SCR mechanisms over CZ and NbCZ catalysts in different temperature ranges.

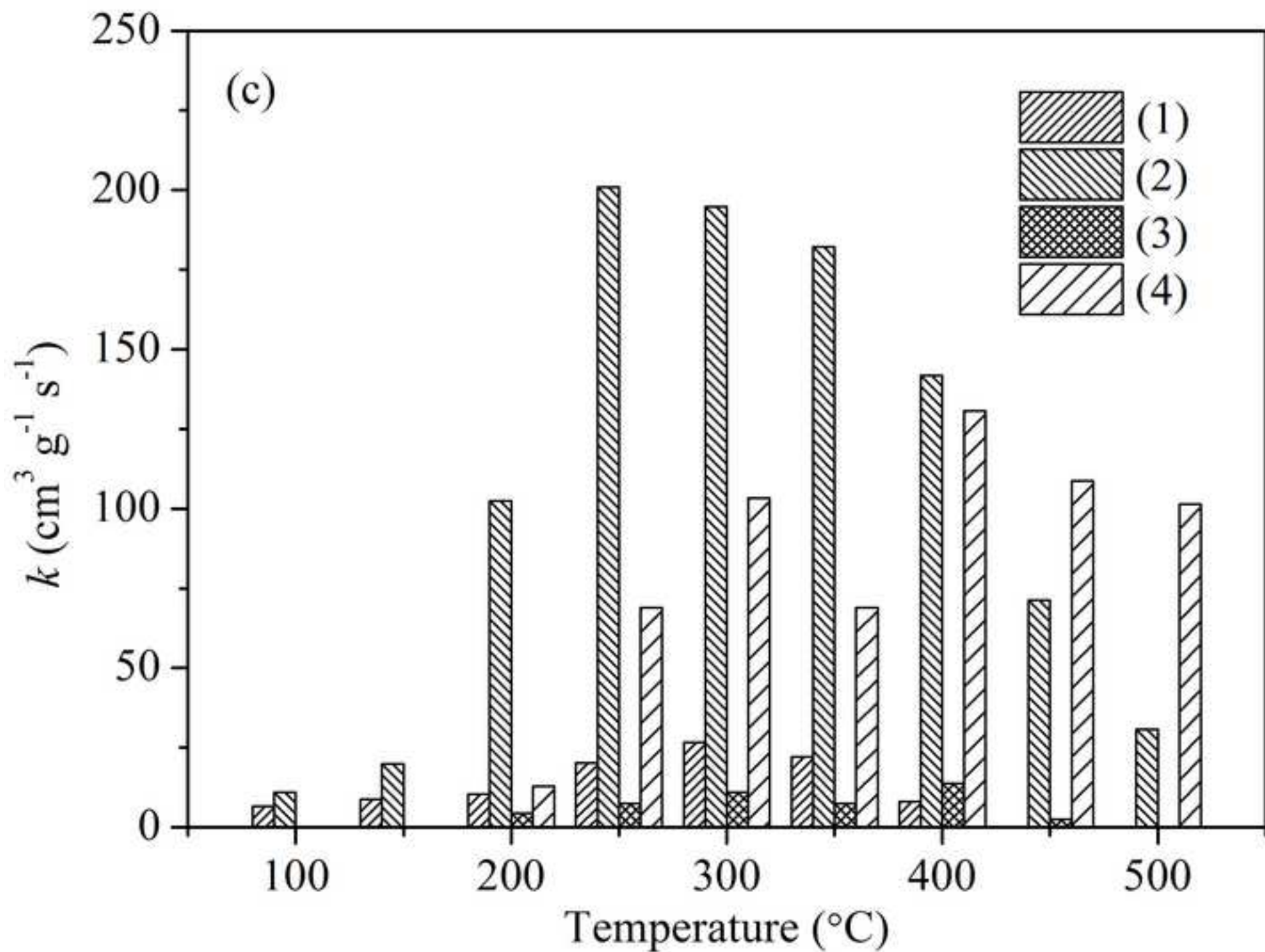
Table 1 Reaction orders for NO and NH₃ concentrations over NbCZ at various temperatures.

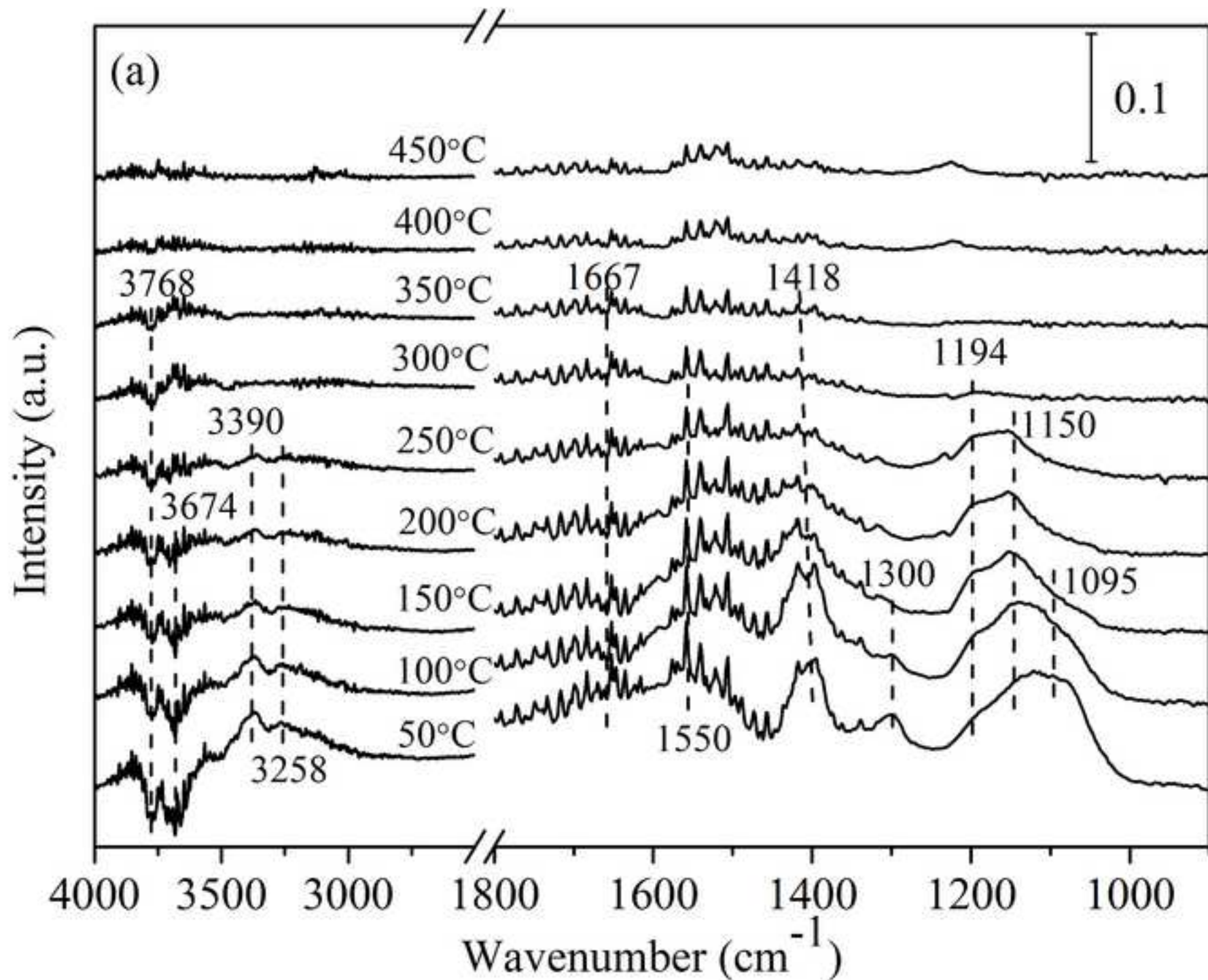
| Temperature (°C) | α | β | |
|------------------|----------|-----------|-----------|
| | | β_1 | β_2 |
| 180 | 0.365 | | -0.177 |
| 200 | 0.738 | | -0.096 |
| 220 | 0.844 | 0.172 | -0.140 |
| 240 | 0.831 | 0.357 | -0.080 |
| 260 | 0.826 | 0.366 | -0.057 |

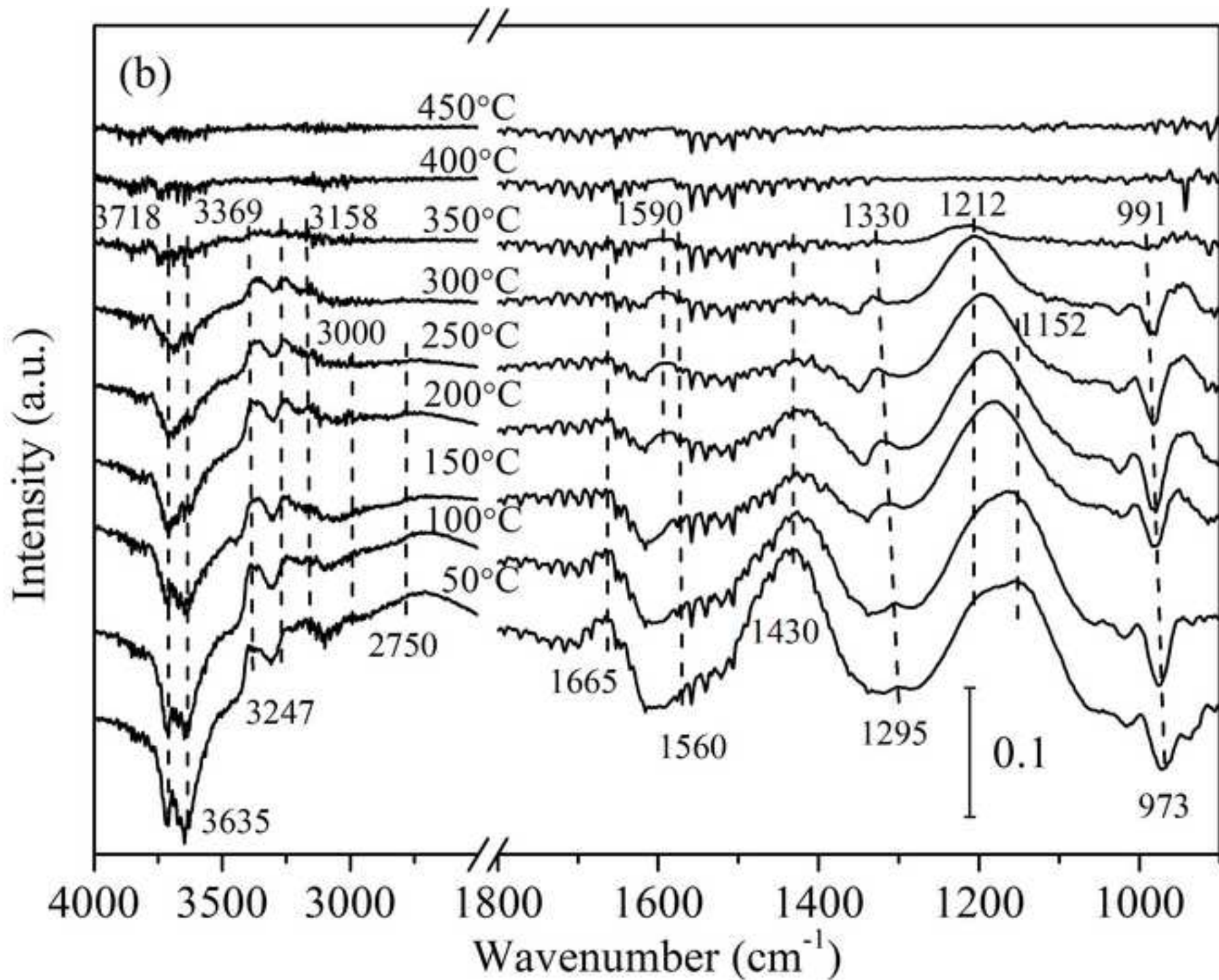
Note: β_1 and β_2 is the reaction order for NH₃ concentration at low and high concentrations, respectively.

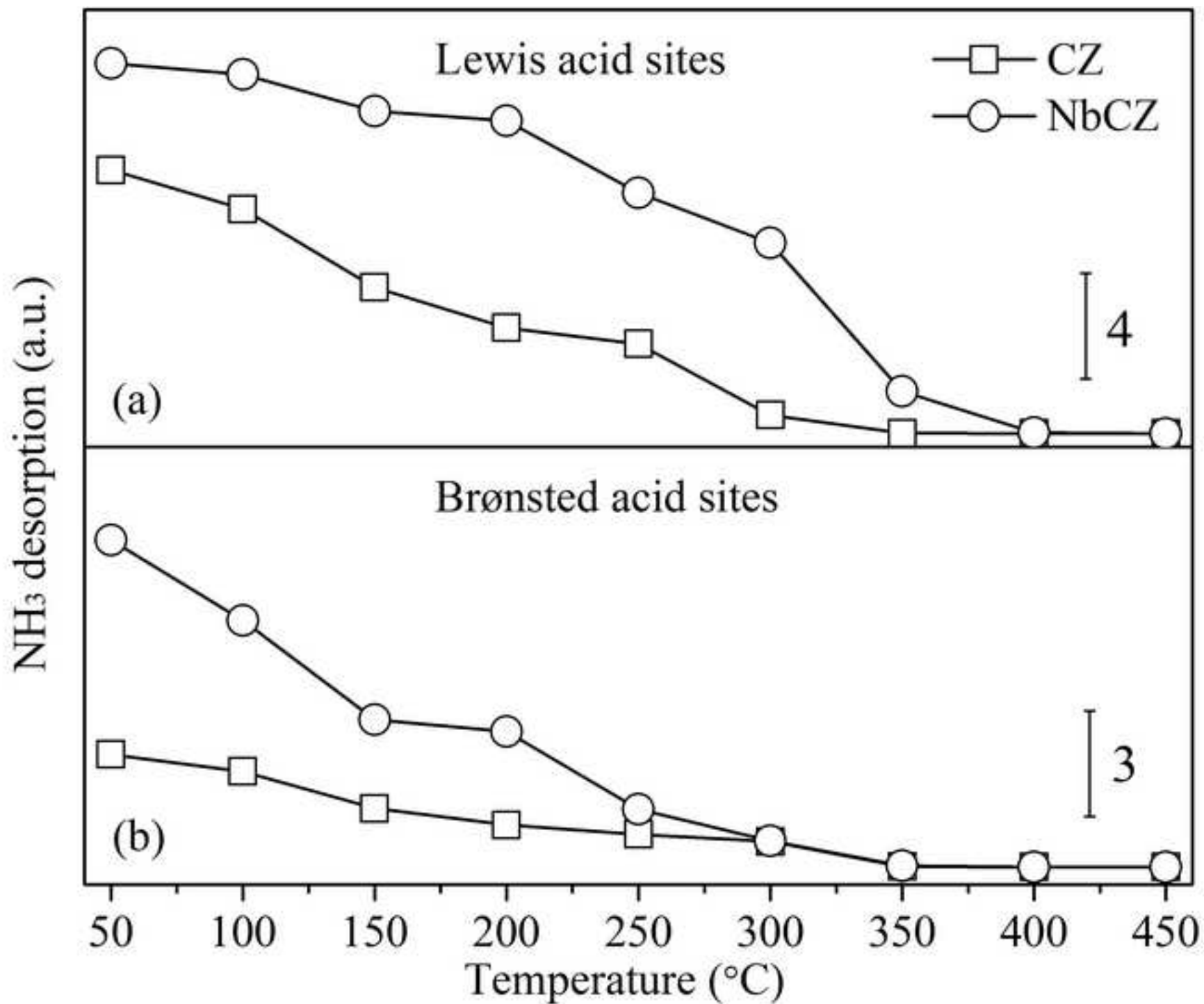


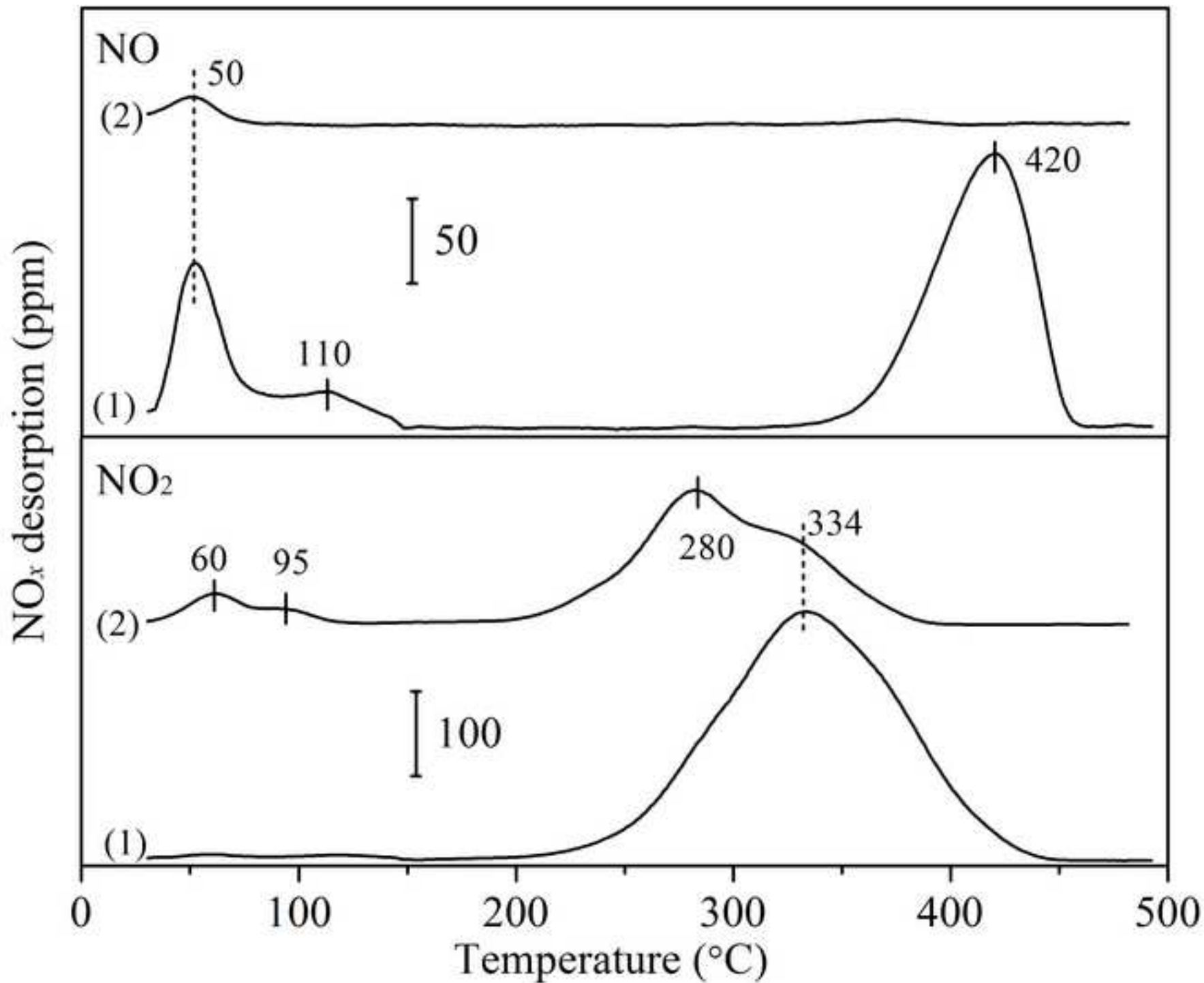


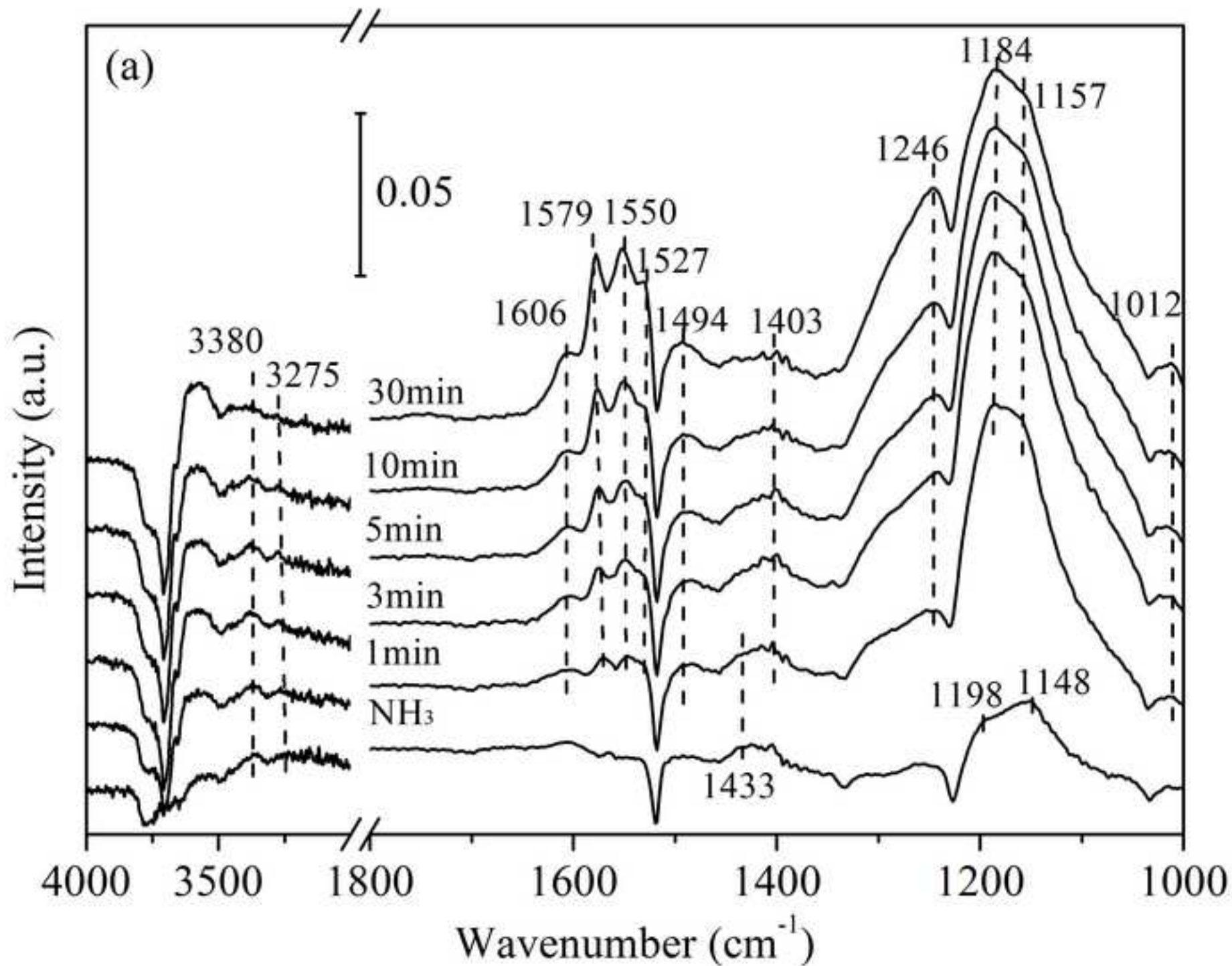


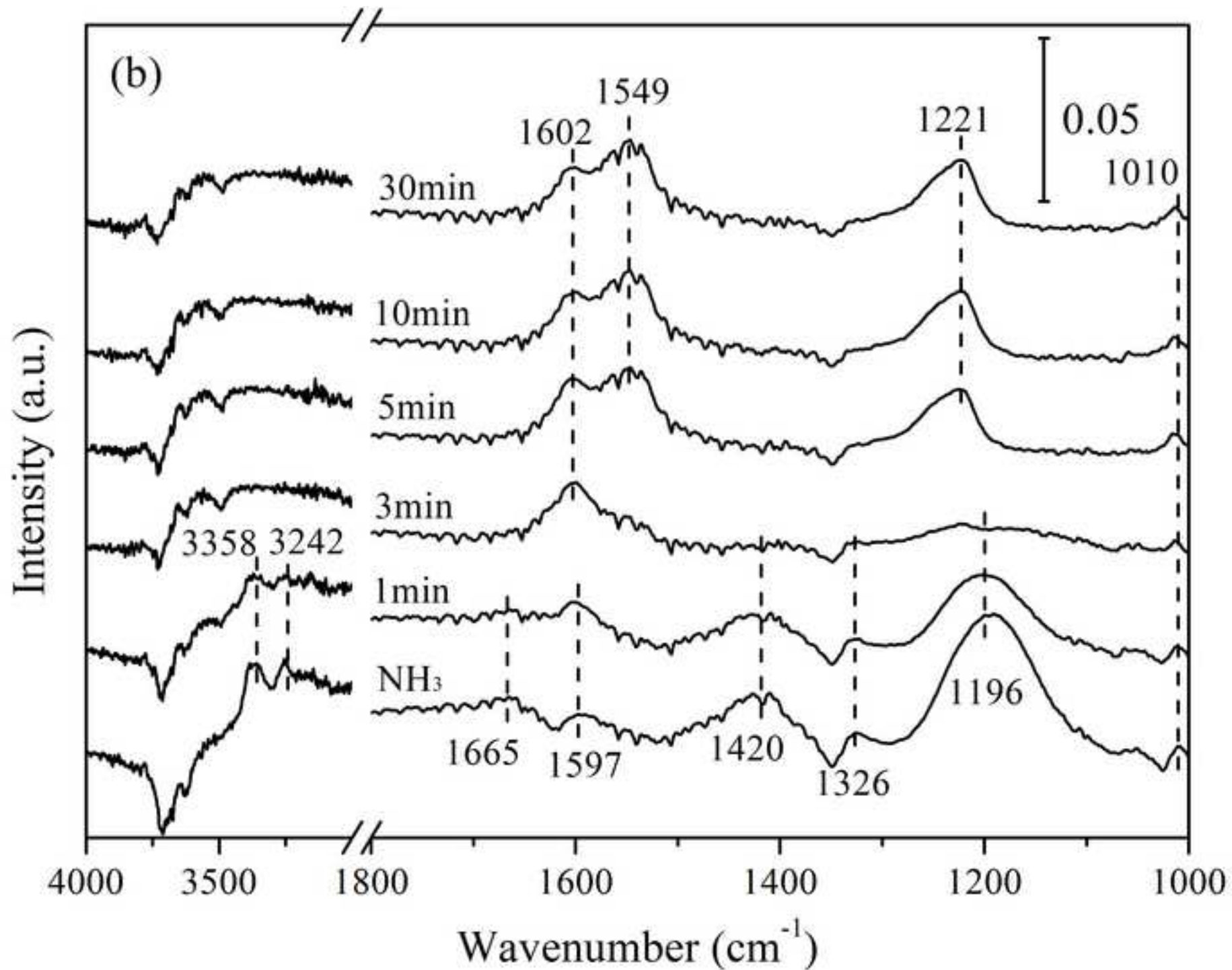


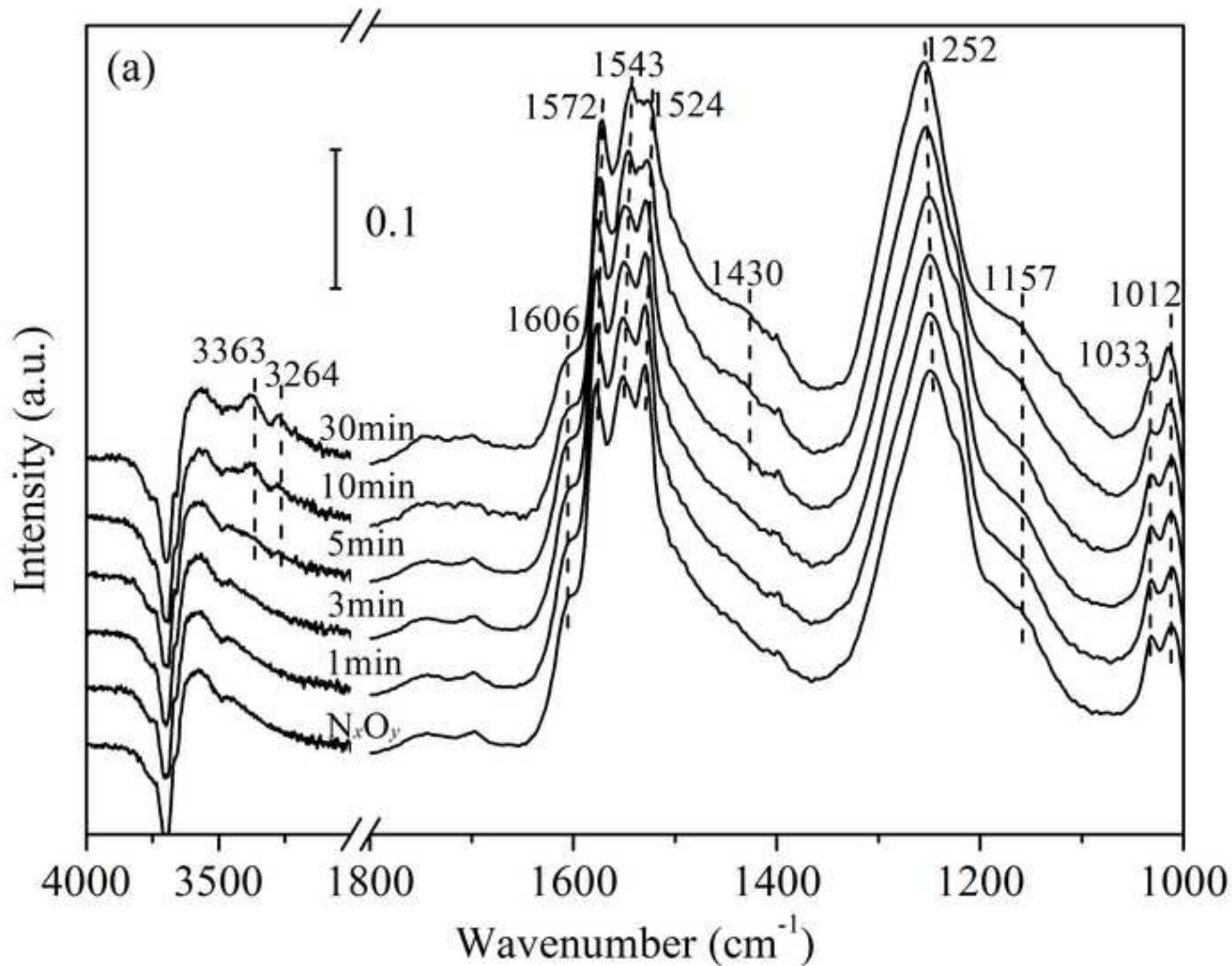


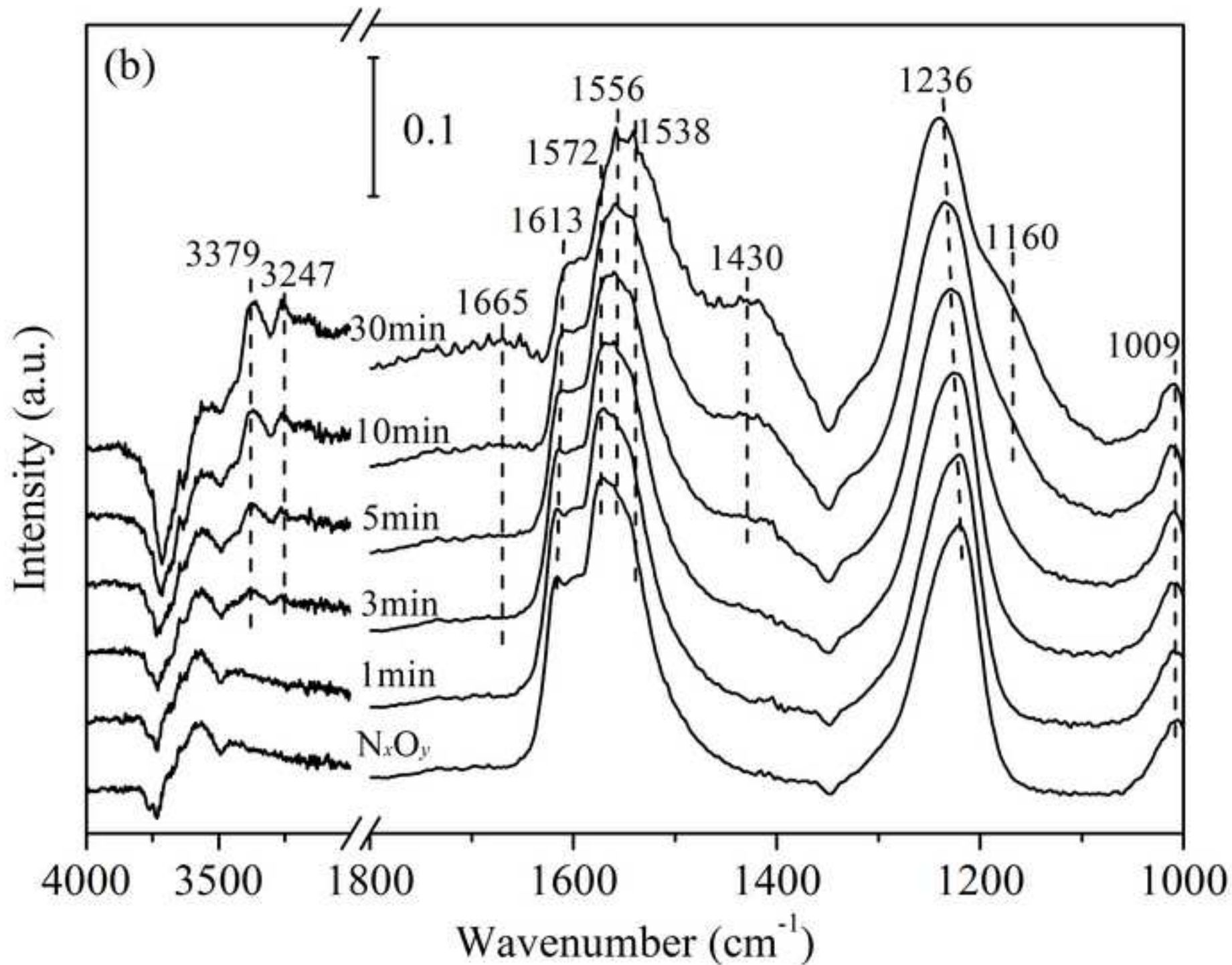


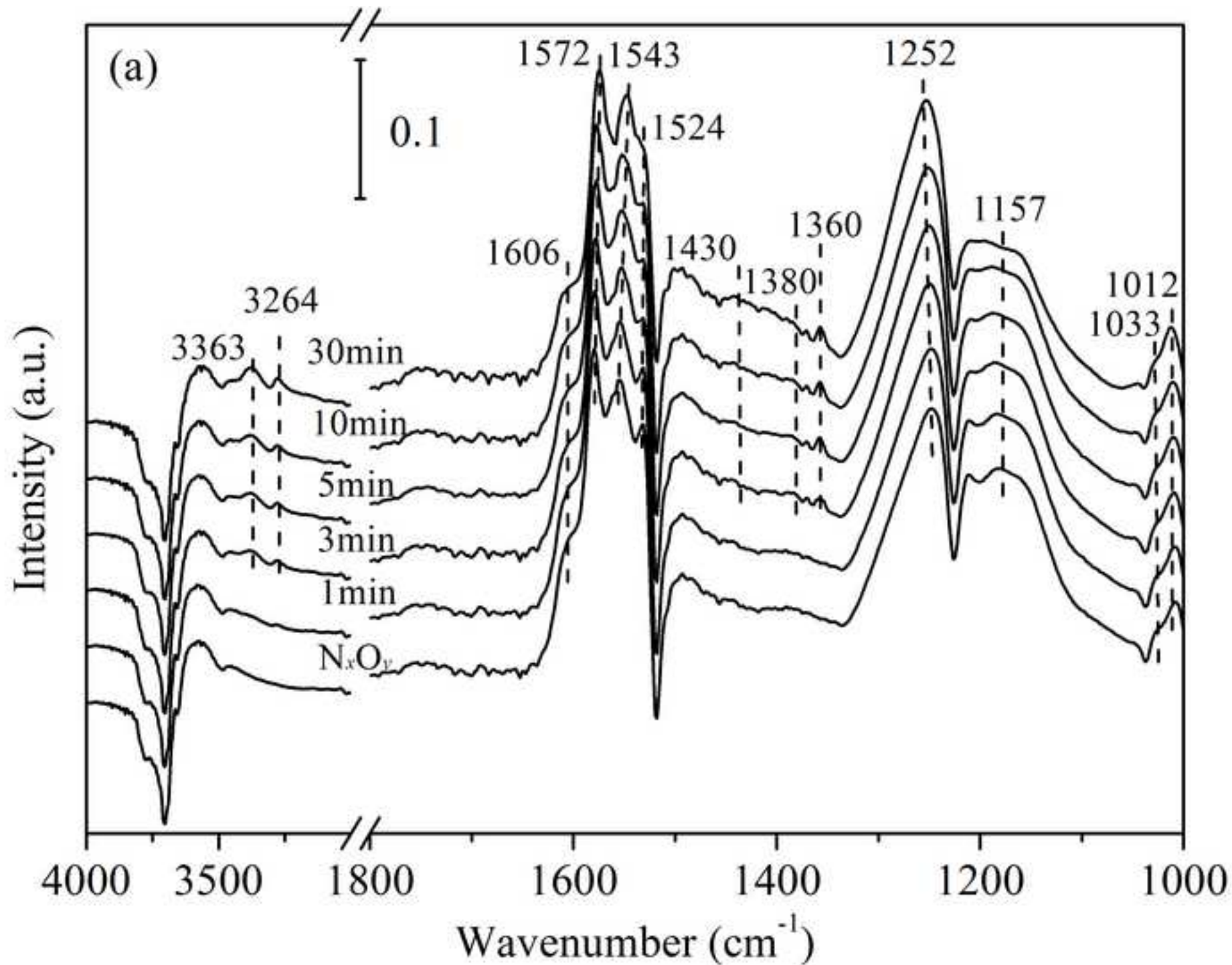


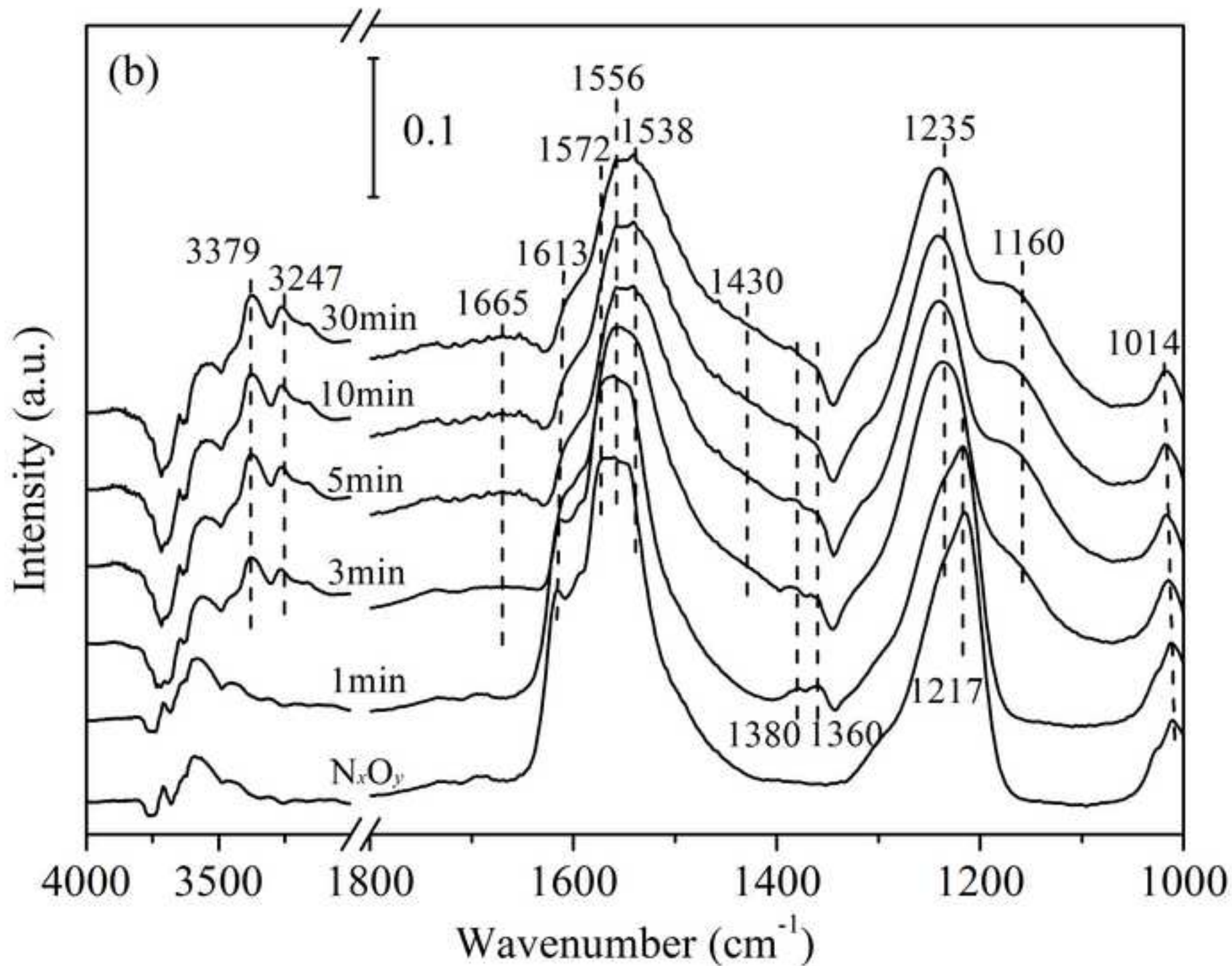


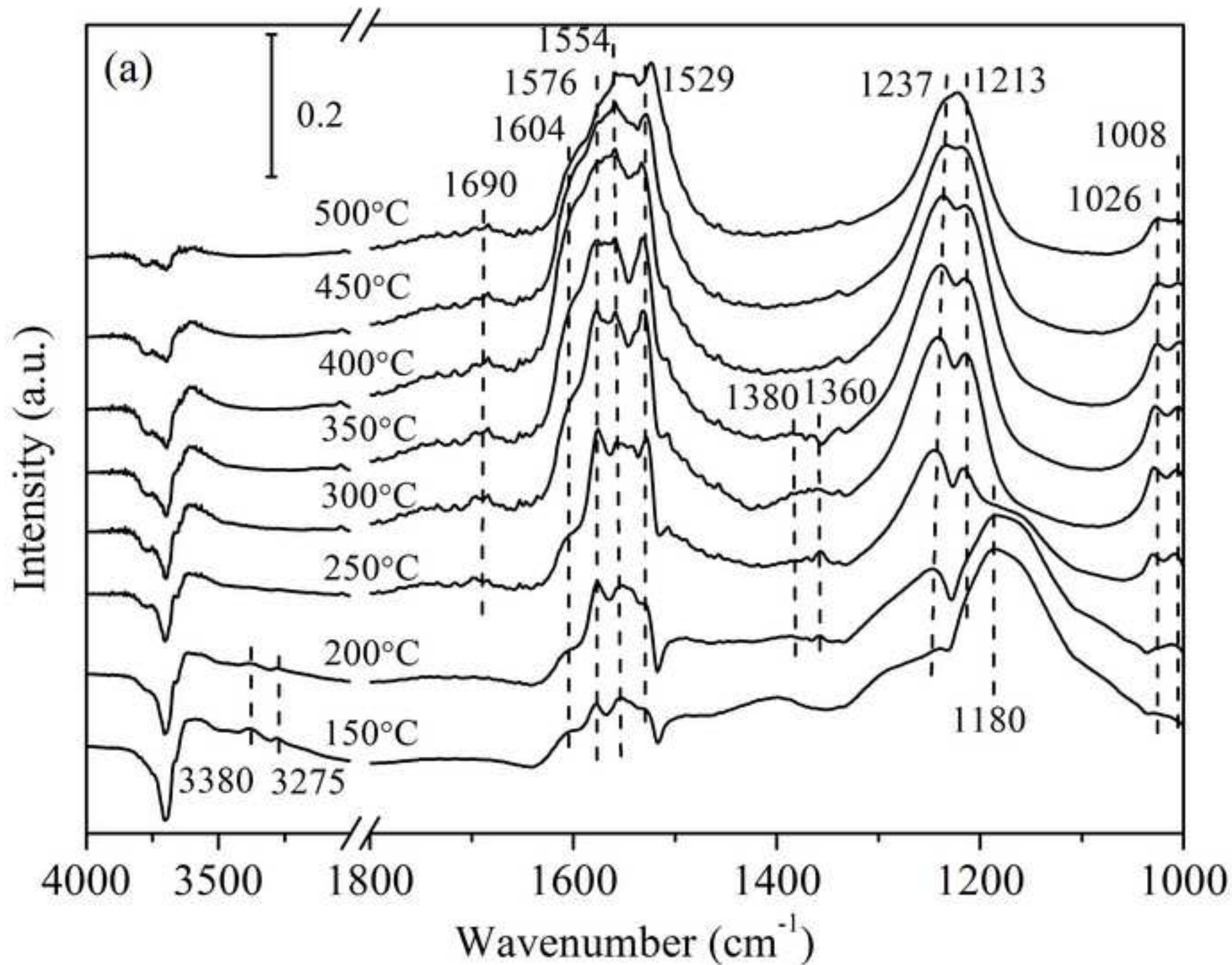


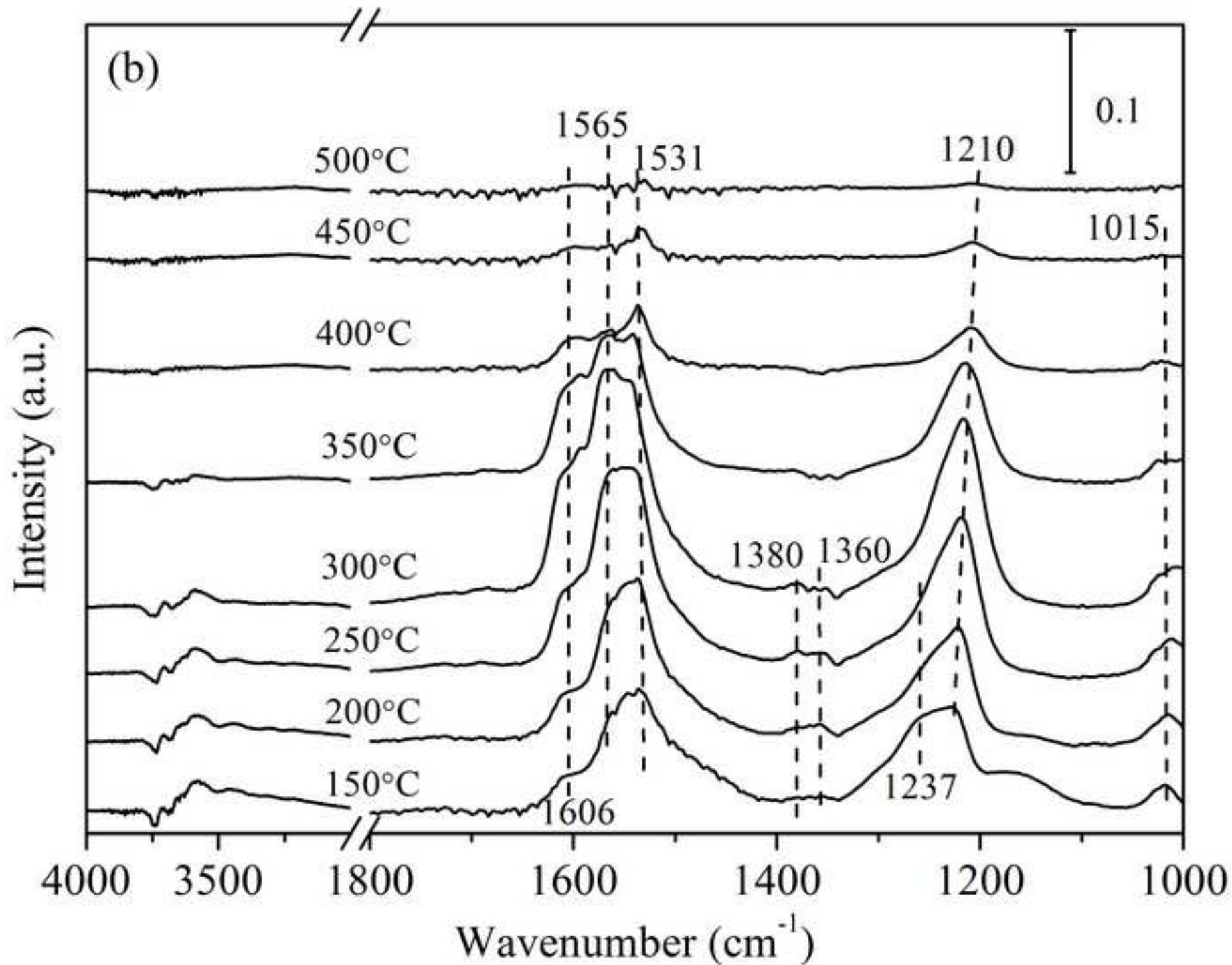


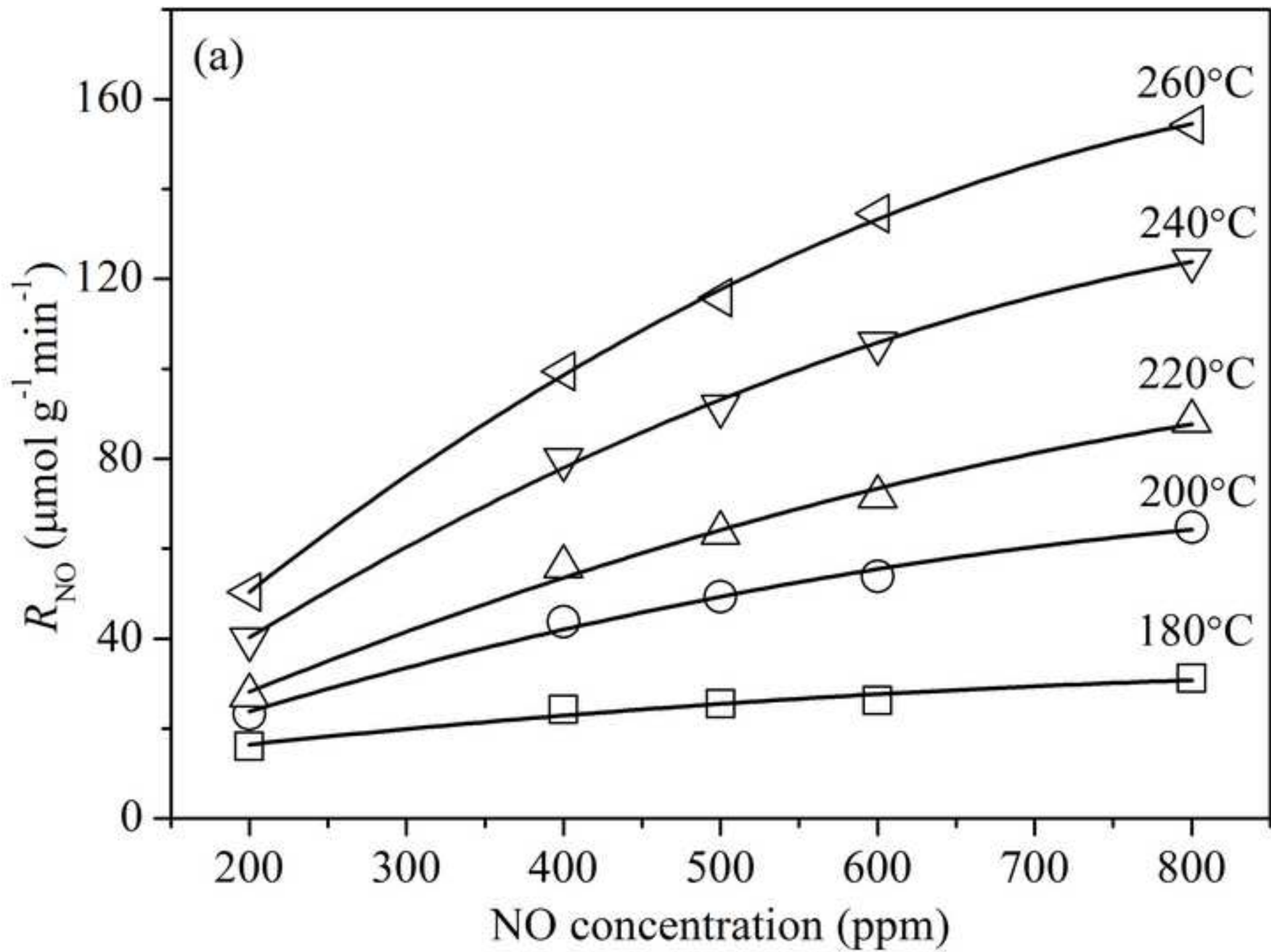


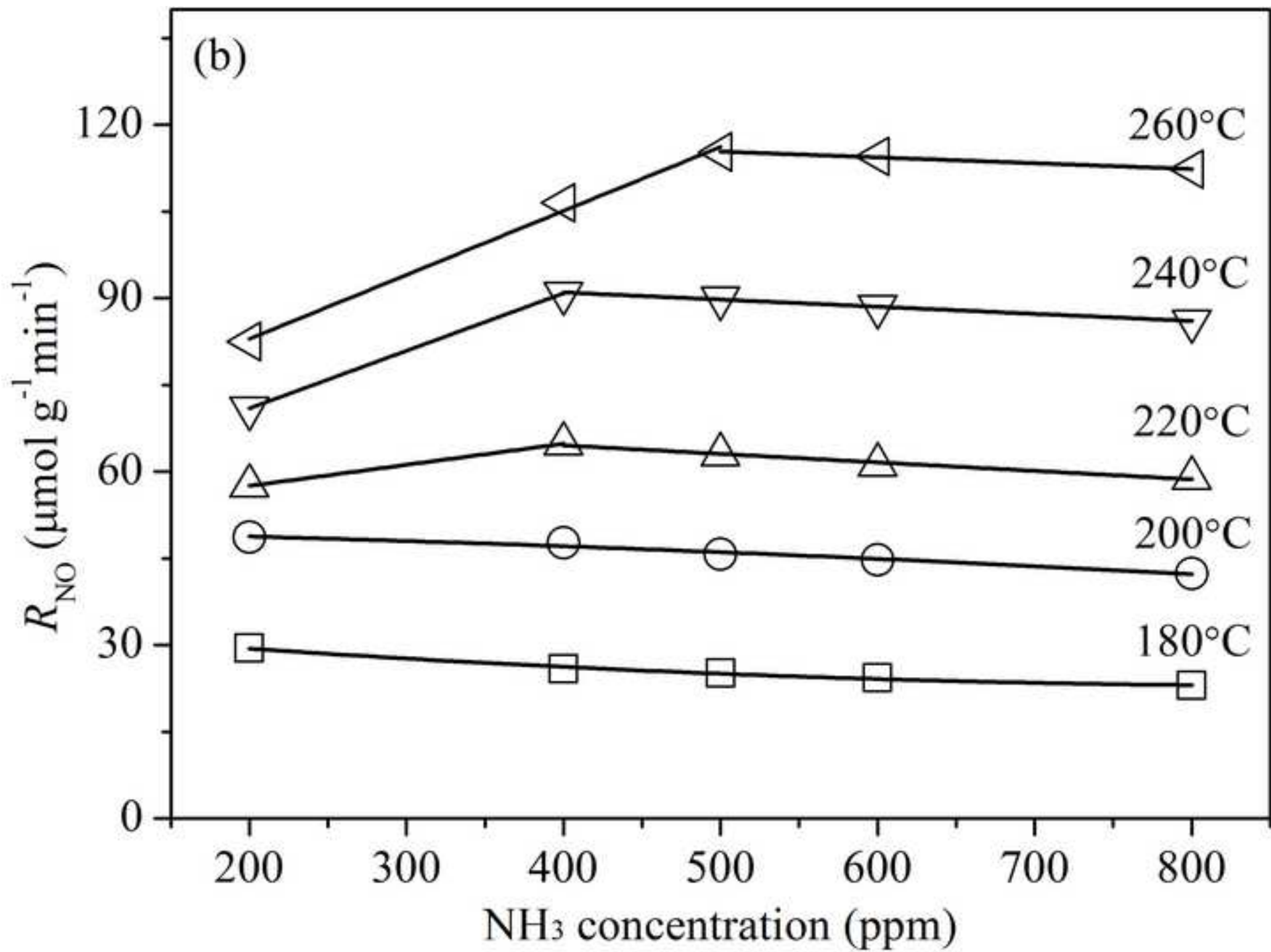


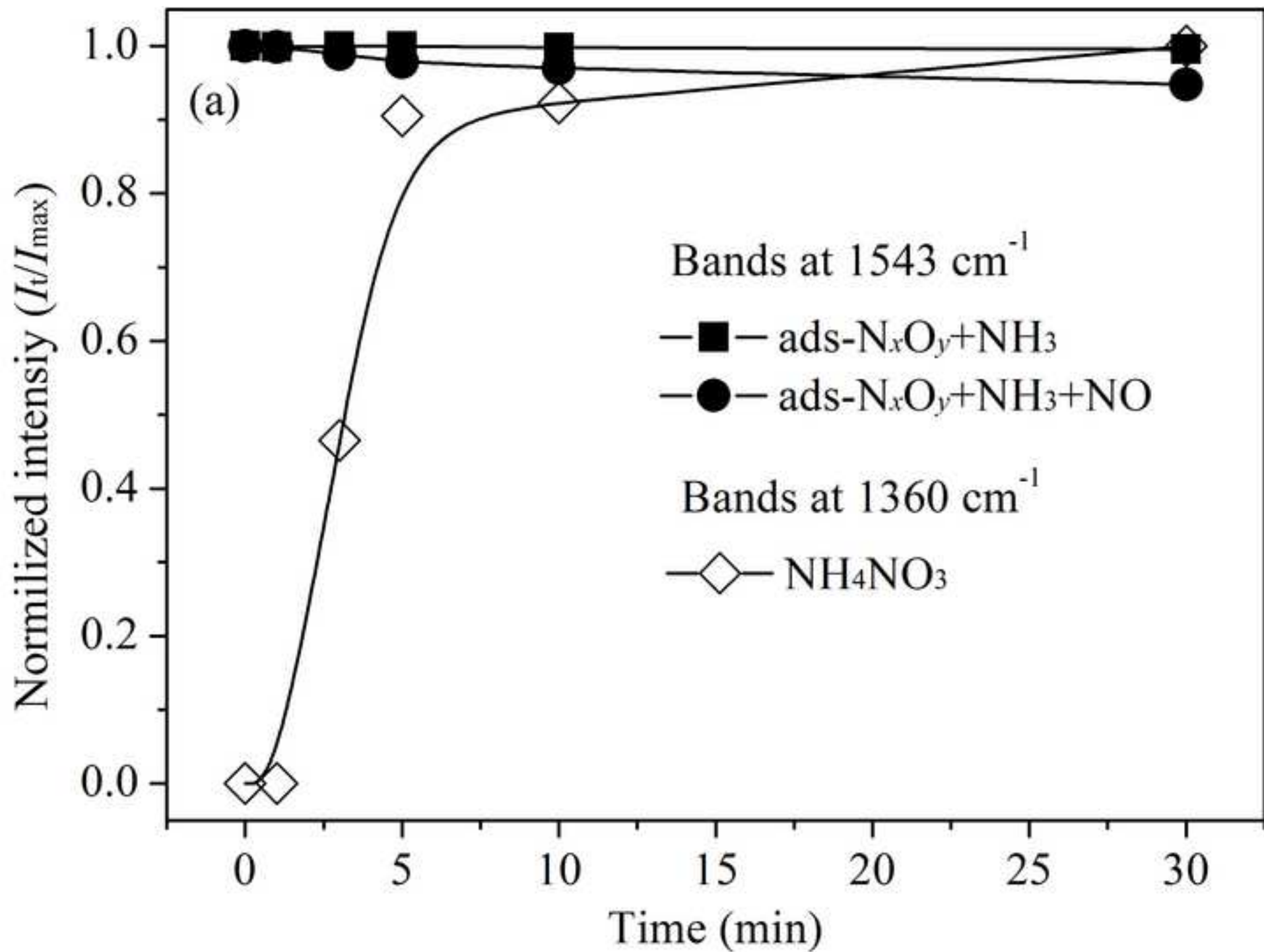


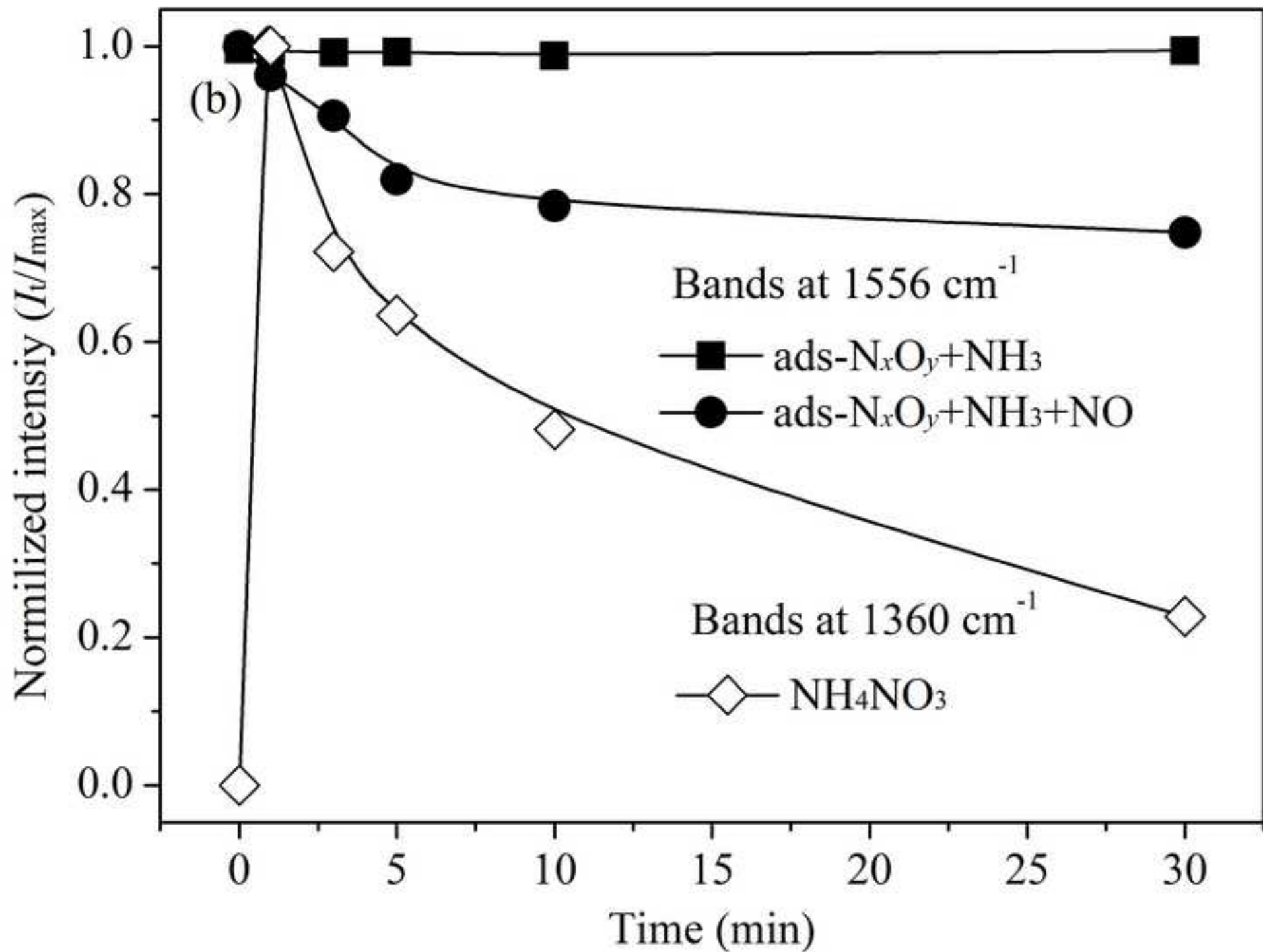




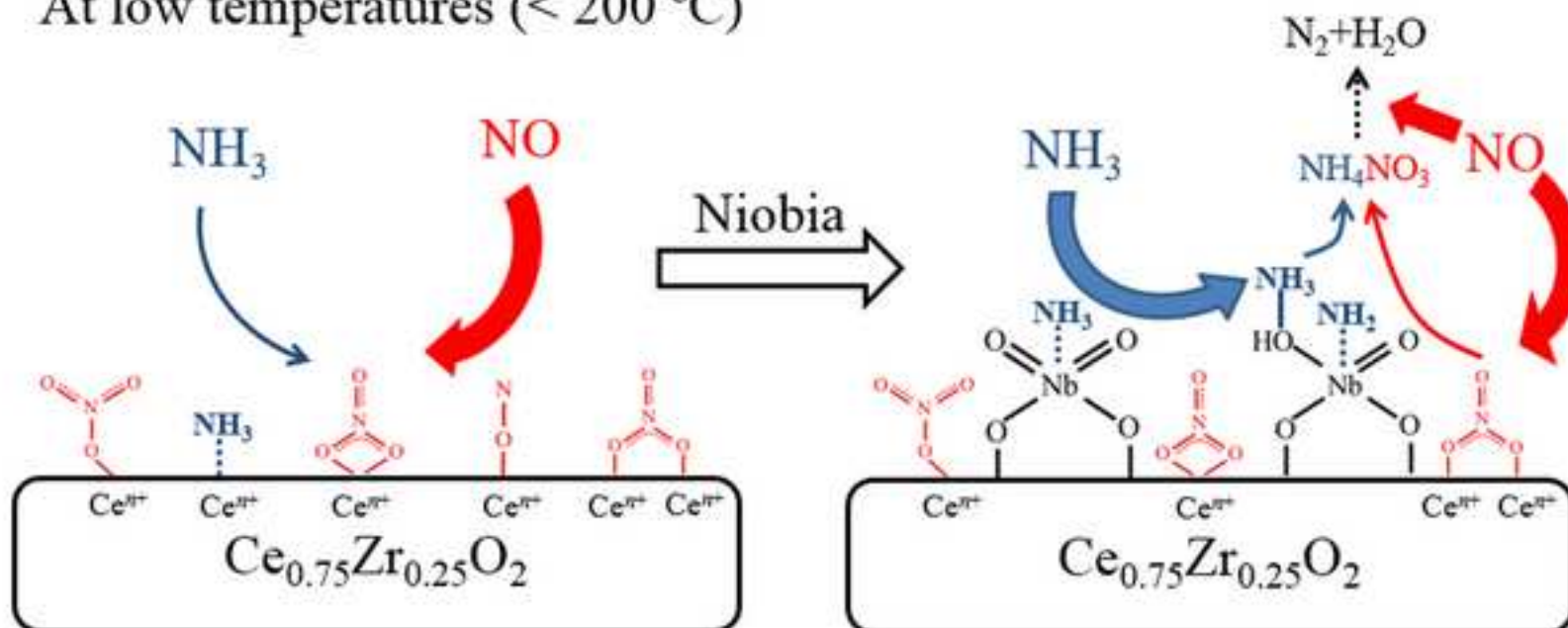








At low temperatures (< 200 °C)



At high temperatures (> 350 °C)

